[1,2,4]Triazolo[1,5-*c*]pyrimidines as Adenosine Receptor Antagonists: Modifications at the 8 Position to Reach Selectivity towards A_3 Adenosine Receptor Subtype

Stephanie Federico,[a] Enrico Margiotta,[b] Veronica Salmaso,[b] Giorgia Pastorin,[c] Sonja Kachler,[d] Karl-Norbert Klotz,[d] Stefano Moro,*[b] and Giampiero Spalluto*[a]

[a]*Dipartimento di Scienze Chimiche e Farmaceutiche, Università di Trieste, Via Licio Giorgeri 1, 34127 Trieste, Italy*

[b]*Molecular Modeling Section (MMS), Dipartimento di Scienze del Farmaco, Università di Padova, via Marzolo 5, 35131 Padova, Italy*

[c]*Department of Pharmacy, National University of Singapore, 3 Science Drive 2, Singapore 117543*

[d]*Institut für Pharmakologie und Toxikologie, Universität Würzburg, Versbacher Strasse 9, 97078 Würzburg, Germany*

To whom correspondence should be addressed.

Tel +39 040 5583726 (G.S.), +39 049 8275704 (S.M.). Fax +39 040 52572 (G.S.), +39 049 8275366 (S.M.). E-mail: spalluto@units.it (G.S.), stefano.moro@unipd.it (S.M.).

Abbreviations: AR, adenosine receptor; cAMP, cyclic adenosine monophosphate; CCPA, 2-chloro-N6-cyclopentyladenosine; CHO, chinese hamster ovary; Cl-IB-MECA, 2-cChloro-N^6-(3-iodobenzyl)-adenosine-5′-*N*-methyluronamide; DBU, 1,8-diazabicyclo[5.4.0]undec-7-ene; HEMADO, 2-(1-hHexynyl)-N^6-methyladenosine; HMDS, hexamethyldisiloxane; IB-MECA, N^6-(3-iIodobenzyl)adenosine-5′-*N*-methyluronamide; MAPK, mitogen-activated protein kinase; NECA, 5'-*N*-ethylcarboxamidoadenosine; PLC, phospholipase C; R-PIA, R-(-)-N6-(2-phenylpropyl)adenosine; TP, [1,2,4]triazolo[1,5-*c*]pyrimidine.

Keywords: G protein-coupled receptor; adenosine receptor; A_3 antagonist; [1,2,4]triazolo[1,5-*c*]pyrimidine; molecular modeling; docking.

Abstract

[1,2,4]Triazolo[1,5-*c*]pyrimidine is a promising platform to develop adenosine receptor antagonists. Here, we tried to investigate the effect of the substituent at the 8 position of [1,2,4]triazolo[1,5-*c*]pyrimidine derivatives on affinity and selectivity at the human A_3 adenosine receptor subtype. In ~~particular~~particular, we have introduced both esters and amides, principally with a benzylic nature. In addition, a small series of 5-substituted [1,2,4]triazolo[1,5-*c*]pyrimidines was designed in order to complete the structure-activity relationship analysis. Several of ~~this~~ these new compounds showed affinity towards ~~hA_3 AR~~human A_3 adenosine receptor in the low nanomolar~~e~~ range, with the most potent derivative of the series bringing a 4-ethylbenzylester at the 8 position (compound **18,** ~~hA_3 AR~~hA_3AR K_i = 1.21 nM). Docking studies performed on the synthesized compounds inside models of human A_1, A_{2A} and A_3 adenosine receptors showed similar binding modes, comparable with the typical crystallographic binding mode of the inverse agonist ZM-241385.

Formattato: Pedice

Formattato: Pedice

Introduction

Adenosine is an endogenous autacoid which carries out its actions by interacting with specific G protein-coupled receptors named adenosine receptors (ARs).[1] Adenosine possesses a double face in pathological conditions: in some cases it can help to resolve or to limit the disease process; while in others, it has a detrimental effect on the pathological event. It is exactly in this second situation that antagonists towards the adenosine receptors could be useful therapeutic agents.[2] Adenosine receptors are divided in four different subtypes: A_1, A_{2A}, A_{2B} and A_3ARs.[3] A_{2A} and A_{2B} ARs are mainly coupled to G_s proteins; on the contrary, A_1 and A_3 ARs are generally coupled to G_i proteins, thus leading to an enhancement or decrease of intracellular cAMP levels, respectively.-[1] Additionally, the various AR subtypes are able to activate other pathways, such as PLC (A_1, A_{2B} and A_3 ARs; A_{2B} and A_3 via G_q coupling) and MAPK (all ARs) pathways.[4] A_1-AR was found also to activate potassium channels and to inactivate calcium (N, P and Q type) channels.[1] AR subtypes showed different organ and tissue distribution in the human body, which confers to them diverse physio-pathological implications. In particular, antagonists for human A_1 AR (hA_1AR) were studied for the treatment of heart and renal failure,[5][6] while Parkinson's disease is the main therapeutic application for hA_{2A}-AR antagonists,~~[7]~~ even if a possible use was suggested also for other neurodegenerative diseases such as Alzheimer's disease and depression,[~~8~~7] and in addiction problems.[8] Concerning hA_{2B}–AR antagonists there is high interest for their potential as drugs in inflammatory conditions such as asthma [9] but also in hypoxic conditions like sickle cell disease.[10] Finally, antagonists towards hA_3–AR were principally proposed for the treatment of glaucoma, but a beneficial effect was suggested also for some kind of cancer and inflammation.[11] For the hA_3–AR subtype, opposite or contradictory results were found in various pathophysiological conditions (i.e. inflammation and cancer), also depending on the species involved.[12] Maybe for these reasons, even though ~~a lot of~~many ligands targeting hA_3–AR are available, only few of them reached the clinical or preclinical phases of experimentation (Figure 1). In particular, the agonist IB-MECA is advancing in phase II and II/III

Formattato: Pedice

for conditions like psoriasis, rheumatoid arthritis and dry eye disease[13] while Cl-IB-MECA is under phase II clinical trial for the treatment of hepatocellular carcinoma, and phase I/II for chronic hepatitis genotype 1.[14] Instead, as antagonists, Palobiofarma compound PBF-677 (structure not disclosed) has recently positively completed a "first in human" phase Ia study to assess safety and tolerability in healthy volunteers.[15]

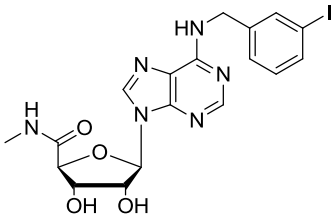

IB-MECA, I
hA_1AR K_i= 51nM
$hA_{2A}AR$ K_i= 2,900 nM
$hA_{2B}AR$ K_i= 11,000 nM
hA_3AR K_i= 1.8 nM

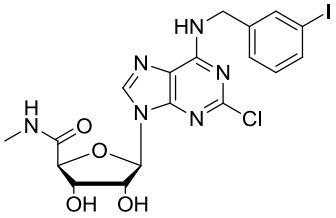

Cl-IB-MECA, II
hA_1AR K_i= 220 nM
$hA_{2A}AR$ K_i= 5,360 nM
$hA_{2B}AR$ K_i> 10,000 nM
hA_3AR K_i= 1.4 nM

Figure 1. hA_3-AR ligands in clinical phases: agonists IB-MECA (**I**) and Cl-IB-MECA (**II**).

In a previous work, we have reported a series of [1,2,4]triazolo[1,5-*c*]pyrimidines (TP) as adenosine receptor antagonists.[16] Concerning the hA_3AR subtype, two compounds emerged from the series: compound **1** and **2** (Figure 2). These compounds bear a methylamino (compound **1**) and ethylamino (compound **2**) ~~moiety~~ moieties at the 5 position of the [1,2,4]triazolo[1,5-*c*]pyrimidine scaffold, respectively. Both of them showed an affinity value towards the hA_3 ~~adenosine receptor~~ AR in the nanomolar range (**1**, hA_3AR K_i = 4.14 nM; **2**, hA_3AR K_i = 3.30 nM), with compound **1** displaying a better selectivity profile against the other AR subtypes (**1**, hA_1/hA_3 = 236; hA_{2A}/hA_3 = 25 *vs* **2**, hA_1/hA_3 = 49; hA_{2A}/hA_3 = 15).

Formattato: Tipo di carattere: Non Grassetto

Formattato: Inglese (Stati Uniti)

Formattato: Tipo di carattere: Corsivo

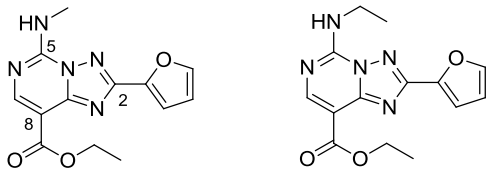

1
hA_3AR K_i= 4.14 nM
hA_1/hA_3= 236
hA_{2A}/hA_3= 25

2
hA_3AR K_i= 3.30 nM
hA_1/hA_3= 49
hA_{2A}/hA_3= 15

Figure 2. Reference [1,2,4]triazolo[1,5-*c*]pyrimidine compounds **1-2**.[16]

The aim of this work was to enhance affinity, but especially, selectivity towards the hA_3AR, maintaining the methylamino moiety at the 5 position of TP and exploring the 8 position through substitution of the ethyl ester moiety with other alkyl or aralkylesters and amides. In addition, a further investigation on the 5 position of TP was performed. In particular, different moieties which share the presence of a second functional group (i.e. amino or ester moieties) where introduced in order to explore their ability to gain new key interactions within the binding site of hA_3-AR.

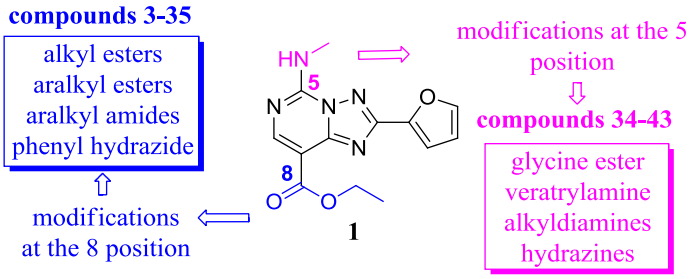

Figure 3. Modifications carried out at the 5 (pink) and 8 (blue) positions of reference compound **1** which led to newly synthesized compounds **3-43**.

Results and Discussion

Chemistry

Designed compounds **3-43** were synthesized as depicted in schemes 1-3, following procedures already reported in literature.[16][17] The synthesis started with the ~~the~~ pyrimidine nucleus (**44**) by reacting S-methylisothioureahemisulfate salt with diethyl ethoxymethylenmalonate in basic conditions. The resulting 5-methylthio-pyrimidine derivative **44** was in turn chlorinated

with phosphorous oxychloride and then reacted with the 2-furoylhydrazide to afford the 4-hydrazinyl-pyrimidine derivative **45**. The last underwent cyclization under dehydrative conditions (hexamethyldisiloxane and phosphorous anhydride in dry xylene) to the TP **46**. At this point, substitution at the 5 position was carried out using methylamine in ethanol and heating to 90-110°C in a sealed tube, yielding compound **1**. Finally, in order to obtain different substitutions at the 8 position, the ethyl ester was hydrolyzed with lithium hydroxide to the corresponding carboxylic acid (**47**), which was in turn reacted with the corresponding alcohol or amine in the presence of phosphorous oxychloride and pyridine affording the desired esters (**3-19**) and amides (**20-32**), respectively (Scheme 1).

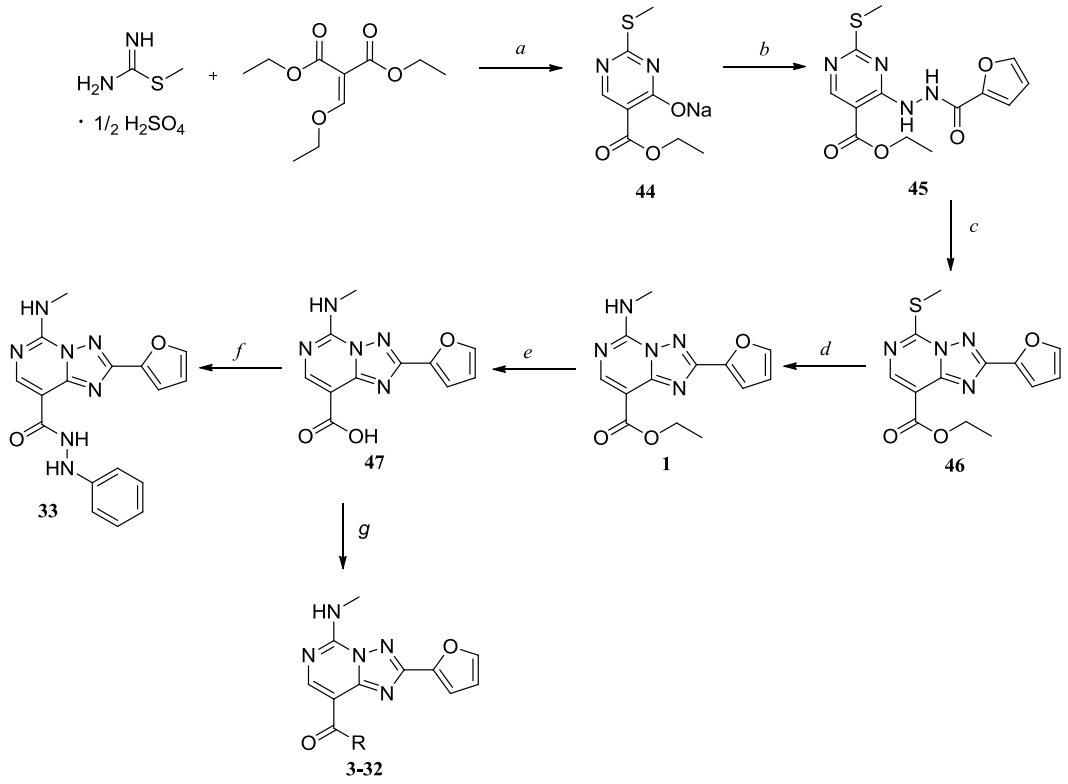

Scheme 1. Synthetic pathway for compounds **3-33**. Reagents and conditions. *a*: NaOH, water, EtOH, rt, 24h; *b*: 1. $POCl_3$, reflux, 3h, 2. 2-furoylhydrazide, DBU, THF, rt, 16h; *c*: P_2O_5, HMDS, xylene, 90°C, 2h, reflux, ~~24~~48h; *d*: NH_2CH_3 33 wt.% in EtOH, EtOH, 120°C in a sealed tube, 3h; *e*: $LiOH \cdot H_2O$, water, EtOH, reflux,

3h;~~–~~ *f*: NH_2NHPh, EDCI, HOBT, EtOH, rt, 16h; *g*: ROH or NH_2R, $POCl_3$, pyr, ~~reflux~~rt, 16h. For R specification of compounds **3-32** see table 1.

The only exception is represented by compound ~~33 which~~**33**, which was obtained by a coupling reaction between acid derivative **47** and phenylhydrazine in the presence of EDCI and HOBT. The same strategy reported in ~~scheme~~ Scheme 1 was applied also to obtain compound **34**: TP **46** was reacted with veratrylamine in ethanol under heating to afford compound **48**, which was hydrolyzed and the obtained acid (**49**) was finally reacted with benzhydryl amine (Scheme 2).

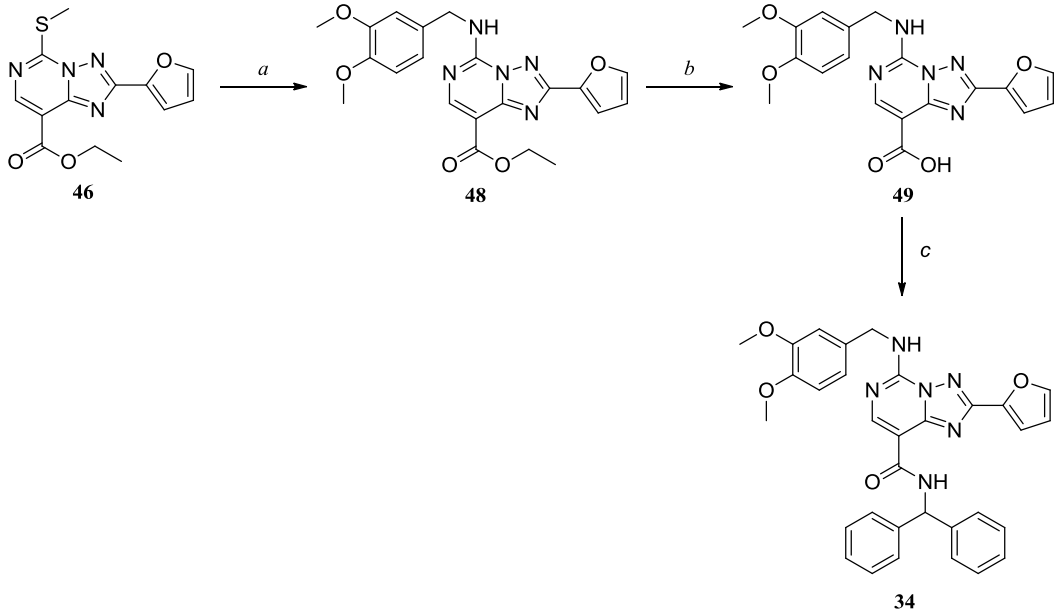

Scheme 2. Synthetic pathway for compound **34**. *a*: NH_2CH_2Ph-3,4$(OCH_3)_3$, EtOH, 120°C in a sealed tube, 3h; *b*: $LiOH{\cdot}H_2O$, water, EtOH, reflux, 3h; *c*: $NH_2CH(Ph)_2$, $POCl_3$, ~~PCl_5,~~ pyr, ~~reflux~~rt, 16h.

Furthermore, in order to obtain the desired compounds ~~35~~**36-39**, the same strategy used for compound **1** was applied, that is a nucleophilic substitution on derivative **46** with the corresponding amines in ethanol at ~~90-11~~120°C. On the other hand, the same reaction using glycine ethyl ester as amine gave both the substitution at the 5 position and the amidation at the 8 position, affording compound **35**. Deprotection with hydrochloric acid in ethyl acetate of Boc-protected derivatives **37-39** afforded ~~then~~ diamino derivatives **40-42** (Scheme 3). Instead, carboxylic acid derivative **43** was obtained from compound **37** analogously to compounds **47**,**49**~~.~~. Finally, compound **50** is a

Formattato: Tipo di carattere: Grassetto

Formattato: Tipo di carattere: Grassetto

secondary product isolated from reactions of derivatives ~~35~~38~~-~~ and **39** in ethanol, which was also characterized and assayed at adenosine receptor subtypes. In fact, the yields for these reactions were low (e.g. **38** = 45%; **39** = 15%), indicating a poor reactivity of the amines used which allowed to ethanol (solvent) to play as reagent for the substitution at the 5 position.

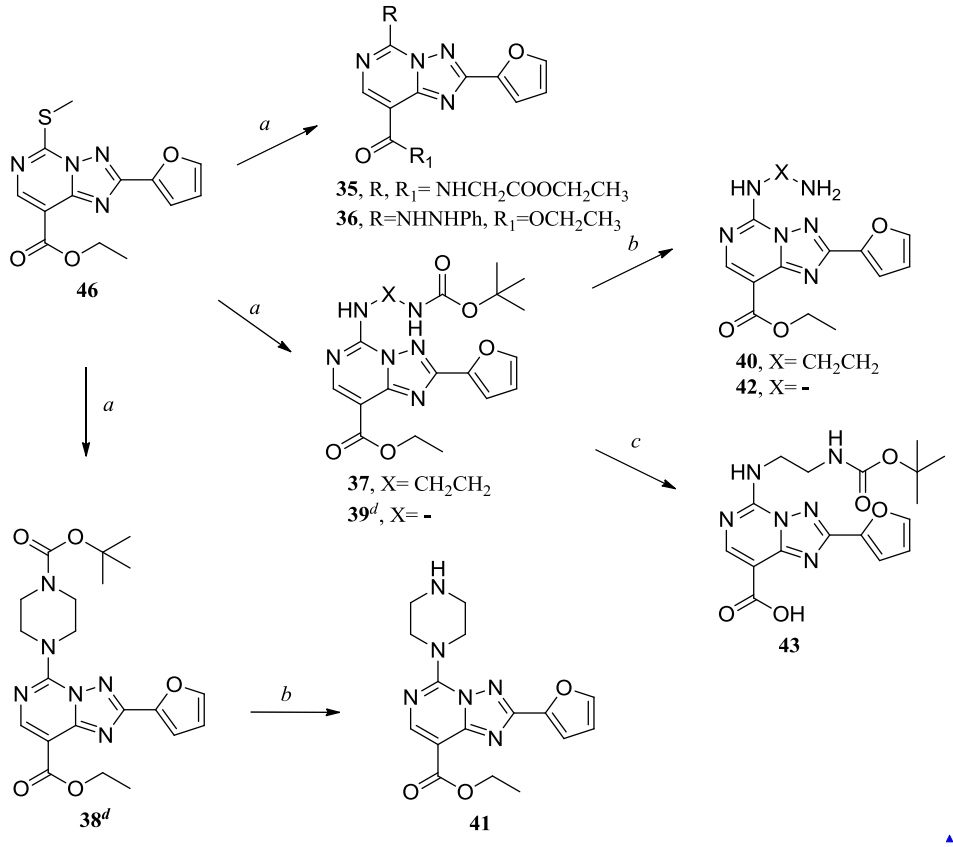

Scheme 3. Synthetic pathway for compounds **35-43**. *a*: appropriate amine ($NH_2CH_2COOEt·HCl$ for **35**, NH_2NHPh for **36**, $NH_2CH_2CH_2NHBoc$ for **37**, N-Boc-Pyperazine for **38**, NH_2NHBoc for **39**), EtOH, 120°C in a sealed tube, 3h; *b*: ~~TFA~~HCl/~~DCM 1:1~~EtOAc, rt, 2h, *c*: LiOH-H_2O, H_2O, EtOH, reflux, 3h~~-~~; *d*: Ethyl 5-ethoxy-2-(furan-2-yl)-[1,2,4]triazolo[1,5-*c*]pyrimidine-8-carboxylate (**50**) was obtained as byproduct.

Pharmacology

All the synthesized compounds **3-43,50** were tested at the four adenosine receptor subtypes.

Formattato: Tipo di carattere: Non Grassetto
Formattato: Tipo di carattere: Grassetto
Formattato: Tipo di carattere: Grassetto
Formattato: Allineato a sinistra
Formattato: Inglese (Regno Unito)
Formattato: Pedice
Formattato: Pedice
Formattato: Tipo di carattere: Corsivo
Formattato: Tipo di carattere: Grassetto

In particular, radioligand binding assays were applied to hA_1, hA_{2A} and hA_3 ARs expressed in CHO cells which afforded affinity values, expressed as K_i for the tested compounds. [^{3}H]CCPA (1 nM), [^{3}H]NECA (10 nM) and [^{3}H]HEMADO (1 nM) were used as radioligands for hA_1, hA_{2A} and hA_3 ARs binding assays, respectively.

Instead, for hA_{2B} AR, potency of newly synthesized compounds was determined using a functional assay, which consists in measurement of the inhibition of NECA-stimulated adenylyl cyclase activity on membranes of CHO cells expressing hA_{2B} AR. ~~In this case, potency of inhibitors was expressed as IC_{50}.~~

Structure-activity relationship

As previously described, the first aim of this work was to explore the 8 position of the [1,2,4]triazolo[1,5-*c*]pyrimidine scaffold by introducing various esters and amides of different nature (e.g. alkyl and aralkyl), while maintaining the methylamino group at the 5 position and the fur-2-yl ring at the 2 position such as in compound **1**, which showed the best affinity/selectivity profile in the previous series. [16] Pharmacological results about synthesized esters and amides **3**-~~34~~ **33** are reported in table 1. In order to better exploit the chemical space around 5 and 8 positions and to explore the effect on selectivity among ARs, compound **34**, bearing big substituents at both positions, was synthesized. In particular, the already reported compound **48**, which bears a veratrylamino group at the 5 position and displayed good affinity and poor selectivity towards hA_3AR was selected as starting point and modified by introduction of the big benzhydrylamido moiety at the 8 position. [16]

Table 1. Binding affinity (hA_1, hA_{2A}, hA_3) and potency (hA_{2B}) of compounds ~~3~~**1**-~~34~~ **35** and ~~50~~ **48** at the four human adenosine receptor subtypes and selectivity towards hA_3AR.

Formattato: Tipo di carattere: Grassetto

Formattato: Tipo di carattere: Grassetto

Formattato: Pedice

Formattato: Inglese (Stati Uniti)

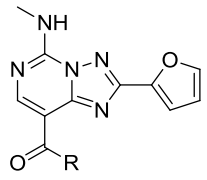

3-33

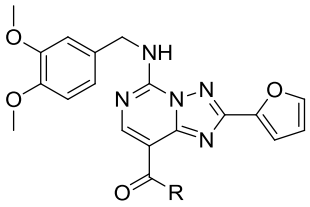

34,48

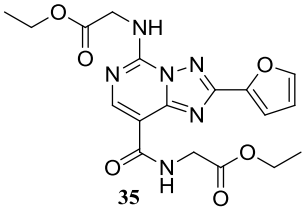

35

Cmpd	R	hA_1-AR (K_i nM)	hA_{2A}-AR (K_i nM)	hA_{2B}-AR (K_i nM)	hA_3-AR (K_i nM)	hA_1/ hA_3	hA_{2A}/ hA_3
1[a]	OEt	978 (716-1,340)	104 (89.2-122)	2,450 (1,770-3,370)	4.14 (3.53-4.86)	236	25
2[a]	OEt	162 (157-167)	50.3 (48.8-51.9)	3,060 (2,230-4,200)	3.30 (2.85-3.83)	49	15
3	$OCH(CH_3)_2$	744 (577-959)	86.5 (63.9-117)	> 3,000	2.75 (2.43-3.12)	270	32
4	OCH_2Ph	277 (220-350)	114 (80.3-161)	> 3,000	7.21 (4.22-12.3)	38	16
5	$OCHPh_2$	48.3 (43.0-54.2)	197 (118-329)	> 10,000	1.99 (1.6-2.47)	24	99
6	OCH_2Ph-2-CH_3	93.9 (73.0-121)	37.2 (29.2-47.4)	> 10,000	30.6 (19.0-49.1)	3	1
7	OCH_2Ph-3-CH_3	79.7 (47.8-133)	21.0 (17.2-25.6)	> 10,000	10.8 (6.92-16.8)	7	2
8	OCH_2Ph-4-CH_3	190 (180-201)	62.2 (36.8-105)	> 10,000	3.72 (3.07-4.50)	51	17
9	OCH_2Ph-2-OCH_3	55.2 (42.0-72.4)	13.2 (8.03-21.8)	> 10,000	1.71 (1.14-2.57)	32	8
10	OCH_2Ph-3-OCH_3	34.3 (28.6-41.0)	14.9 (10.5-21.0)	≈1,000	7.42 (5.51-9.99)	5	2
11	OCH_2Ph-4-OCH_3	102 (79.9-131)	194 (111-337)	> 10,000	5.62 (4.73-6.67)	18	35
12	OCH_2Ph-2-Cl	348 (249-485)	32.0 (23.8-43.2)	> 10,000	6.05 (4.61-7.95)	58	5
13	OCH_2Ph-3-Cl	26.4 (15.1-46.2)	15.7 (13.5-18.4)	≈10,000	6.73 (4.06-11.2)	4	2
14	OCH_2Ph-4-Cl	216 (195-238)	71.9 (61.1-84.5)	> 10,000	4.88 (3.03-7.86)	44	15
15	OCH_2Ph-2-Br	313 (231-423)	24.3 (21.1-27.9)	> 10,000	14.3 (6.56-31.2)	22	2
16	OCH_2Ph-3-F	130 (93.5-181)	32.5 (26.5-39.9)	> 10,000	3.37 (1.99-5.73)	39	10
17	OCH_2Ph-4-F	556 (316-980)	71.5 (58.2-87.8)	> 10,000	5.21 (4.30-6.32)	107	14
18	OCH_2Ph-4-CH_2CH_3	119 (79.1-178)	21.0 (17.2-25.6)	> 10,000	1.21 (0.907-1.62)	98	17
19	$OCH(CH_3)Ph$	51.0 (35.3-73.8)	11.0 (6.83-17.6)	3,720 (1,980-6,990)	3.19 (2.06-4.93)	16	3
20	$NHCH_2Ph$	23.4 (19.0-28.9)	18.6 (10.8-32.1)	> 10,000	3.73 (3.00-4.65)	6	5

Formattato: Inglese (Stati Uniti)

Tabella formattata

Formattato: Inglese (Stati Uniti)

Formattato: Tipo di carattere: Non Grassetto, Corsivo, Apice

Formattato: Inglese (Stati Uniti)

Formattato: Inglese (Stati Uniti)

Formattato: Tipo di carattere: Non Grassetto

Formattato: Inglese (Stati Uniti)

Formattato: Inglese (Stati Uniti)

Formattato: Inglese (Stati Uniti)

Formattato: Inglese (Stati Uniti)

Formattato: Inglese (Stati Uniti)

Formattato: Inglese (Stati Uniti)

Formattato: Inglese (Stati Uniti)

Formattato: Inglese (Stati Uniti)

Formattato: Inglese (Stati Uniti)

Formattato: Inglese (Stati Uniti)

Formattato: Inglese (Stati Uniti)

Formattato: Inglese (Stati Uniti)

Formattato: Inglese (Stati Uniti)

21	$NHCHPh_2$	28.3 (20.5-39.1)	61.6 (52.3-72.5)	≈10,000	5.08 (4.53-5.70)	6	12
22	$NHCH_2Ph$-4-CH_3	46.6 (41.5-52.4)	100 (75.6-132)	> 10,000	5.02 (3.9-6.46)	9	20
23	$NHCH_2Ph$-4-OCH_3	41.0 (29.3-57.3)	81.3 (60.3-110)	> 10,000	12.5 (9.9-15.8)	3	7
24	$NHCH_2Ph$-4-CF_3	3,850 (2,430-6,090)	2,950 (1,930-4,500)	> 10,000	15.3 (11.6-20.1)	252	193
25	$NHCH_2Ph$-4-Cl	137 (110-169)	59.4 (50.8-69.4)	> 10,000	10.0 (9.58-10.5)	14	6
26	$NHCH_2Ph$-4-F	250 (228-274)	47.6 (39.8-56.8)	> 10,000	7.23 (5.96-8.77)	35	7
27	$NHCH_2Ph$-4-Ph	> 100,000	9,390 (8,600-10,300)	> 10,000	521 (341-797)	>191	18
28	$NHCH_2Ph$-3,4$(OCH_3)_2$	246 (166-365)	141 (106-187)	> 10,000	102 (90.2-115)	2	1
29	$NH(CH_2)_2Ph$	73.1 (47.8-112)	29.7 (27.1-32.6)	> 10,000	6.82 (5.10-9.12)	11	4
30	$NH(CH_2)_2Ph$-3,4$(OCH_3)_2$	177 (121-259)	169 (105-271)	> 10,000	107 (91.4-124)	2	2
31	$NHC(CH_3)_2CH_2Ph$	38.0 (30.0-48.0)	6.12 (5.92-6.33)	> 3,000	6.52 (4.40-9.66)	6	1
32	$NH(CH_2)_2OPh$	172 (165-180)	38.2 (28.0-52.2)	> 10,000	16.4 (10.5-25.7)	10	2
33	NH-NH-Ph	58.7 (54.2-63.6)	342 (286-408)	> 10,000	15.1 (13.3-17.2)	4	23
34	$NHCHPh_2$-	122 (77.0-193)	137 (115-163)	> 30,000	69.9 (46.8-105)	2	2
35	-	21,900 (21,500-22,300)	1,540 (1,090-2,170)	> 10,000	646 (524-797)	34	2.4
504	OEt	4,100315 (2,79003-6,020489)	1,86016 (1,45144.3-2,387305)	> 1013,00030	10838.7 (94.428.2-12453.1)	38	173
8[a]				0 (7,950-22,200)			

[a] data from reference 16.

All the derivatives (**3-354**) displayed good affinities at the hA_3AR with different degrees of selectivity *versus* the other receptor subtypes, while they were inactive~~, in the nanomolar range,~~ towards the $hA_{2B}AR$ receptor (K_i> 3,000 nM for all compounds except for compound **10**). Instead, at the hA_1 and hA_{2A} AR subtypes, substitution at the 8 position on the TP nucleus was able to modulate affinity and consequently also selectivity against hA_3-AR.

In the ester ~~series~~series, an improvement of affinity towards the hA_1-AR was observed with the increase of the size of the ester substituent. The affinity order i~~was~~s: benzhydryl (**5**) ≥ α-

Formattato: Non Evidenziato
Formattato: Inglese (Regno Unito)
Formattato: Inglese (Regno Unito)
Formattato: Inglese (Regno Unito)
Formattato: Inglese (Regno Unito)
Formattato: Inglese (Regno Unito)
Formattato: Inglese (Regno Unito)
Formattato: Inglese (Regno Unito)
Formattato: Inglese (Regno Unito)
Formattato: Tipo di carattere: Non Grassetto
Formattato: Inglese (Regno Unito)
Formattato: Tipo di carattere: Non Grassetto
Formattato: Tipo di carattere: Non Grassetto

methylbenzyl (**19**) >> benzyl (**4**) >> isopropyl (**3**) > ethyl (**1**). In particular, benzhydryl (**5**) and α-methylbenzyl (**19**) derivatives showed affinity values of 48.3 and 51.0 nM, respectively. Introduction of a methyl (but also ethyl such as for compound **18**) or methoxy substituent on the phenyl ring of benzyl ester derivative **4** improved the affinity at the hA_1AR (compounds **6-11**). In detail, substitution at the *meta* position gave the best results (**7**, hA_1-AR K_i= 79.7 nM; **10**, hA_1AR K_i=34.3 nM), followed by substitutions at the *ortho* (**6**, hA_1AR K_i= 93.9 nM; **9**, hA_1AR K_i= 55.2 nM) and *para* positions (**8**, hA_1AR K_i= 190 nM; **11**, hA_1AR K_i= 102 nM). A different behaviour was observed when a halogen atom was introduced in the benzyl ester group (compounds **12-17**). In fact, the substitution with halogens did not necessarily lead to an improvement of affinity at the hA_1 AR. For example, *ortho* chlorine (**12**, hA_1AR K_i= 348 nM) and bromine (**15**, hA_1AR K_i= 313 nM) derivatives displayed a worse affinity than unsubstituted derivative **4** (hA_1AR K_i= 277 nM). Compound **13** (*meta*-chlorine) is the most potent benzyl ester compound at the hA_1-AR with a K_i of about 26.4 nM. Regarding the amide series (**20-34**), it could be observed that while the benzylester (**4**) was poorly active at the hA_1AR, the benzylamide derivative (**20**) displayed a K_i of 23.4 nM at the ~~hA_1 AR~~same receptor (about ten-fold more potent). This affinity value was comparable to that showed by the benzhydrylamide derivative **21** (hA_1AR K_i= 28.3 nM). Also the α-dimethyl-phenylethylamide (**31**, hA_1AR K_i=38 nM) gave good results in terms of affinity at the hA_1AR, while the corresponding not branched phenylethylamide (**29**) and the longer phenoxyethylamide (**32**) derivatives had a detrimental effect (**29**, hA_1AR K_i= 73.1 nM and **32**, hA_1AR K_i= 172 nM). Regarding substitutions on the benzyl group of derivative **20**, only the *para* position was investigated (compounds **22-27**). The introduction of a moiety at this position led to a decrease of affinity at the hA_1-AR, especially when halogen atoms were present (**24-26**). The same behaviour was observed in the veratrylamido derivative **28** (hA_1AR K_i= 246 nM). Finally, also the replacement of methylene in the benzyl derivative **20** with an amino group as in the phenylhydrazide derivative **33** was detrimental in terms of affinity towards the hA_1AR (**20**, hA_1AR K_i= 23.4 nM *versus* **33**, hA_1 K_i= 58.7 nM). ~~In conclusion, it is interesting to note that compound **50**,~~

Formattato: Non Apice / Pedice

~~which bears an ethoxy group at the 5 position of TP instead of an ethylamino group of reference compound **2**, showed a complete loss of affinity against hA_1 AR (hA_1 K_i= 4,100 nM), suggesting that the amino group at the 5 position is involved in crucial interactions inside the hA_1 AR binding pocket.~~

In general, in the ester series (**3-19**) affinities were better towards the hA_{2A}AR than towards hA_1AR and the affinity trend was not related to the size of ester substituent. In fact, the order of affinity values i~~was~~: α-methylbenzyl (**19**) >> isopropyl (**3**) >ethyl (**1**) > benzyl (**4**) >>benzhydryl (**5**). Substitution on the phenyl ring of the benzylester **4** led to an improvement of affinity at the hA_{2A}-AR (compounds **6-18**), excepted for the *para*-methoxy derivative **11** (**4**, hA_{2A}AR K_i= 114 nM *versus* **11**, hA_{2A}AR K_i= 194 nM). *Meta* and *ortho* susbtitutions were preferred to *para* substitution (i.e. **6**, hA_{2A}AR K_i= 37.2 nM and **7**, hA_{2A}AR K_i= 21 nM *versus* **8**, hA_{2A}AR K_i= 62.2 nM). Similarly, regarding amide series (**20-34**), unsubstituted benzylamide group (**20**, hA_{2A}AR K_i= 18.6 nM) was preferred over substituted benzylamido moieties as present in compounds **22-28** (i.e. **22**, hA_{2A}AR K_i= 100 nM). The introduction of a phenylethyl (**29**), phenoxyethyl (**32**) or benzhydryl (**21**) amido group at the 8 position of TP led to a slight decrease of affinity at the hA_{2A}-AR compared to the benzylamido group (i.e. **32**, hA_{2A}AR K_i= ~~18~~38.~~6~~ 2 nM *versus* **20**, hA_{2A}AR K_i= ~~38~~18.~~2~~ 6 nM). On the contrary, α-dimethyl-phenylethylamido derivative **31** showed the best affinity value towards A_{2A}AR, with a K_i value of 6.12 nM.

Concerning the hA_3AR subtype, which is the target of this work, most of the synthesized derivatives displayed affinity values below 30 nM. The isopropyl derivative **3** exhibited a slightly better affinity and selectivity against hA_3AR than the corresponding ethyl ester **1** (**3**, hA_3AR K_i=2.75 nM *versus* **1**, hA_3AR K_i= 4.14 nM). Among arylalkyl esters, benzylester (**4**) led to a decrease of affinity toward hA_3-AR (**4**, hA_3AR K_i= 7.21 nM) which was gained again with bulkier esters such as α-methyl-benzyl (**19**, hA_3AR K_i= 3.19 nM) and benzhydryl esters (**5**, hA_3AR K_i= 1.99 nM). In general, the substitution on the phenyl ring of the benzyl group of compound **4** conferred an improvement in affinity towards the hA_3AR. A particular relationship between affinity

and the position of the substituent on the phenyl ring was not observed. The only observation that could be made is that *para*-substitutions (**8,11,14,17,18**) led to an increase of affinity at the hA_3-AR compared to the unsubstituted derivative **4** (i.e. **18**, hA_3AR K_i= 1.21 nM *versus* **4**, hA_3AR K_i= 7.21 nM), independent of the nature of the substituent. ~~Also, s~~Selectivity against the other adenosine receptor subtypes was better in the *para*-substituted benzyl ester derivatives (**8,11,14,17,18**) than in the other benzyl-susbtituted compounds (**8**, hA_1/hA_3= 51, hA_{2A}/hA_3= 17, *versus* **7**, hA_1/hA_3= 7, hA_{2A}/hA_3=2) as well. Instead, in the amide series (**20-34**), the benzylamido group (compound **20**) gave an affinity at the hA_3AR of 3.73 nM and substitutions on the phenyl ring led to a detrimental effect in terms of affinity at the hA_3AR (**22-28**), especially when a big moiety such as another phenyl ring was introduced at the *para* position (**27**, hA_3AR K_i= 521 nM). Interestingly, when a *para*-trifluoromethyl-benzylamido group was introduced at the 8 position of TP (**24**), the affinity at hA_3-AR was 15.3 nM, thus was less potent than reference compound **1** (hA_3AR K_i= 4.14 nM), but selectivity against both hA_1 and hA_{2A} ARs was good. In fact, compound **24** was 252- and 193- fold selective for hA_3-AR versus hA_1 and hA_{2A} ARs, respectively. ~~Also~~In addition, elongation of the amide chain such as for compounds **29-32** did not improve affinity at the hA_3-AR. Surprisingly, the phenylhydrazide moiety was well tolerated at this receptor subtype. In fact, derivative **33** showed an affinity of 15 nM at the hA_3-AR, which was four-fold less potent than benzylamido compound **20**, but more than four-fold selective against hA_{2A}-AR (**33**, hA_3AR K_i= 15.1 nM, hA_1/hA_3= 4, hA_{2A}/hA_3= 23 *versus* **20**, hA_3AR K_i= 3.73 nM, hA_1/hA_3= 6, hA_{2A}/hA_3= 5). Both affinity and selectivity were completely lost when a bigger moiety than a methylamino group was introduced at the 5 position of compound ~~5~~**21**, such as in compound **34** (hA_3AR K_i= 69.9 nM, hA_1/hA_3= 2, hA_{2A}/hA_3= 2). Comparing compound **34** to its parent compound **48** it is possible to observe that substitution of the ethyl ester with a big amido moiety does not enhance selectivity versus hA_3AR. In fact, compound **34** is actually two fold less potent at this receptor subtype than derivative **48**. A worst behaviour in terms of affinity was observed when the less bulky ethyl glycine ester was

Formattato: Tipo di carattere: Grassetto

Formattato: Tipo di carattere: Grassetto

Formattato: Pedice

Formattato: Tipo di carattere: Grassetto

Formattato: Tipo di carattere: Grassetto

introduced at the 5 position and on the carboxylic acid at the 8 position in compound **35** (hA_3AR K_i= 646 nM).

Most importantly, the introduction of both, different esters and amides at the 8 position of the TP compared to that present in the reference compound **1**, led in general to a decrease of selectivity against hA_1 and hA_{2A} ARs. An exception, as described before, was represented by isopropyl ester derivative **3** which displayed a slight improvement in both affinity and selectivity for the hA_3-AR (hA_3AR K_i= 2.75 nM, hA_1/hA_3= 270, hA_{2A}/hA_3= 32), but selectivity against hA_{2A}-AR remained poor. Unfortunately, if an improvement of both, affinity at the hA_3–AR and selectivity against $hA_{2A}AR$ was obtained, a detrimental effect was observed regarding selectivity against hA_1 AR, such as for compound **5**, which bears the benzhydryl ester group at the 8 position of TP (**5**, hA_3AR K_i= 1.99 nM, hA_1/hA_3= 24, hA_{2A}/hA_3= 99).

In order to better define the structure-activity relationship of TP at the hARs, also additional substitutions at the 5 position of the TP scaffold (compounds ~~35~~36-**43**) were investigated which were not considered in the previous work.[16] In particular, moieties containing an additional functional group such as another amino group or a carboxylic group were introduced to explore the opportunity to gain other key electrostatic interactions inside the hA_3-AR binding cleft which could confer an enhancement of both, affinity and selectivity for the targeted AR subtype. In addition, these substituents could be considered as spacers containing a site of linkage for other possible functionalizing moieties, such as fluorophores, that can be useful in the study of the physiopathological role of hA_3–AR.[18][19] Pharmacological results about compounds ~~35~~36-**43** were reported in table 2.

Table 2. Binding affinity (hA_1, hA_{2A}, hA_3) and potency (hA_{2B}) of compounds **1-2,** ~~35~~36-**43, 50** at the four human adenosine receptor subtypes and selectivity towards hA_3AR.

Formattato: Tipo di carattere: Grassetto

Formattato: Tipo di carattere: Grassetto

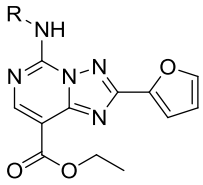

36-37,39,40,42

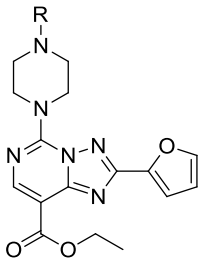

38,41

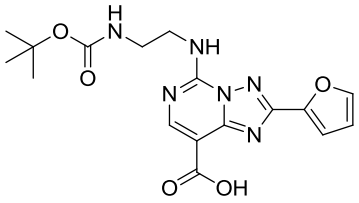

43

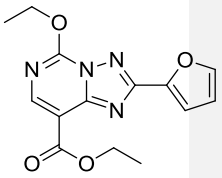

50

Cmpd	R	hA_1AR (Ki nM)	$hA_{2A}AR$ (Ki nM)	$hA_{2B}AR$ (Ki nM)	hA_3AR (Ki nM)	hA_1/hA_3	hA_{2A}/hA_3
1[a]	CH_3	978 (716-1,340)	104 (89.2-122)	2,450 (1,770-3,370)	4.14 (3.53-4.86)	236	25
2[a]	CH_2CH_3	162 (157-167)	50.3 (48.8-51.9)	3,060 (2,230-4,200)	3.30 (2.85-3.83)	49	15
~~35~~	~~CH_2CO_2Et~~	~~21,900 (21,500-22,300)~~	~~1,540 (1,090-2,170)~~	~~> 10,000~~	~~646 (524-797)~~	~~34~~	~~2.4~~
36	NHPh	1,360 (1,060-1,740)	41.8 (35.9-48.8)	6,060 (4,140-8,910)	339 (235-488)	4	0.1
37	$CH_2CH_2NHCO_2C(CH_3)_3$	> 100,000	376 (337-420)	> 30,000	129 (124-133)	>775	2.9
38	$CO_2C(CH_3)$	> 100,000	> 100,000	> 10,000	> 30,000	-	-
39	$NHCO_2C(CH_3)_3$	12,100 (11,800-12,300)	827 (674-1,010)	> 10,000	89 (63.5-125)	136	9.3
40	$CH_2CH_2NH_2$	2,340 (1,880-2,900)	829 (772-890)	> 30,000	2,000 (1,620-2,480)	1.2	0.4
41	H	> 100,000	> 30,000	> 10,000	28,600 (9,710-84,300)	>3.5	>1
42	NH_2	2,080 (1,360 3,190)	63.1 (49.3 80.7)	> 10,000	159 (128-199)	13	0.40
43	-	> 100,000	22,600 (17,800-28,800)	> 30,000	7,750 (7,580-7,910)	>13	2.9
50	-	4,100 (2,790-6,020)	1,860 (1,451-2,387)	> 10,000	108 (94.4-124)	38	17

[a] data from reference 16.

As could be seen, not only ~~aminoester (35) and~~ diamino (**36,40-42**) compounds, but also the mono-Boc protected diamino derivatives (**38,39,43**) were tested for their affinity against the ARs. All derivatives showed a loss of affinity against the hA_3–AR subtype. A free amino group at the 5 position was not tolerated (**40,41**) for substituents bigger than hydrazine (**42**). In fact, hydrazine derivative **42** was the only derivative with a free amino group which exhibited an affinity value in

Formattato: Non Apice / Pedice

Formattato: Tipo di carattere: Non Grassetto, Corsivo, Apice

Tabella formattata

the sub-micromolar range (hA_3AR K_i= 159 nM). The presence of a Boc moiety on the second amino group led to a more potent and selective compound towards hA_3 AR (**39**, hA_3AR K_i= 89 nM), while a phenyl group was less well tolerated (**36**, hA_3AR K_i= 339 nM). Also, the Boc-ethylendiamino chain gave some affinity at the hA_3 AR (**37**, hA_3AR K_i= 129 nM), but the corresponding acid derivative **43** was 60-fold less potent (**43**, hA_3AR K_i= 7,750 nM), confirming that an ester (or amido) moiety was essential at the 8 position of TP in order to obtain affinity in the nanomolar range against this AR subtype.

Finally, compound **50**, which bears an ethoxy group at the 5 position of TP instead of an ethylamino group of reference compound **2**, showed a loss of affinity against all ARs, suggesting that the amino group at the 5 position is involved in crucial interactions inside the binding pocket.

Formattato: Rientro: Prima riga: 0 cm

Formattato: Inglese (Regno Unito)

Molecular modeling

Molecular docking simulations were performed with the aim to rationalize binding at a molecular level. The compounds were docked to the hA_1, hA_{2A} and hA_3 adenosine receptor subtypes, while disregarding the hA_{2B} receptor, since none of the compounds showed significant interaction with this receptor (Ki-> 3000 nM). As reported in the methods section, a crystallographic structure was retrieved from the Protein Data Bank for hA_1 (PDB ID: 5UEN [20]) and hA_{2A} (PDB ID: 3PWH [21]) subtypes, while a homology model constructed on the 3PWH hA_{2A}AR structure was employed for the hA_3 receptor. 3PWH structure was chosen because the ionic interaction between E169 and H264 is lacking, leaving more space for the placement of the compounds (especially for the substituted amine at position 5). Poses with positive electrostatic potentials and highly positive van der Waals interactions (higher than 50 kcal/mol) were rejected; in the case of some non-binders or low affinity binders it was not possible to satisfy this condition (compounds **8** on hA_1, **27** and **50** on hA_{2A}, **38** on hA_3), but the pose with the lowest energy contribution was retained also for these compounds for completeness. In the other cases, a single pose was chosen for each ligand by visual inspection, in a way to optimize the ligand-protein interaction network.

Formattato: Non Apice / Pedice

According to the selected poses, the ligands bind to the three AR subtypes in a similar fashion, comparable with the typical crystallographic binding mode of the inverse agonist ZM-241385, as summarized in Videos S1-2-3. Electrostatic and hydrophobic interactions were computed for each compound and each receptor at a per residue level; the results, plotted in the form of heat maps called Interaction Energy Fingerprints (Figures 4-5-6, panels A and B), highlight conserved hot spots in the three receptor subtypes. These zones are focused on the upper portion of transmembrane helices TM2, TM3, TM6 and TM7, and on extracellular loop EL2. In particular, significant hydrophobic interactions are common to two apolar residues at positions 2.64 and 3.32, leucine 3.33, a phenylalanine in EL2, tryptophan 6.48, leucine 6.51, isoleucine 7.39; while a strong electrostatic interaction is found at level of asparagine 6.55.

The main interactions of conserved and non-conserved residues are reported by the histograms in panels C of Figures 4-5-6: the strength of the interactions at equivalent positions of the three AR subtypes is shown to highlight how single point differences among the receptors could affect binding. Data are reported for compounds **5**, **9** and **18**, the ligands with highest affinity for hA_3AR; and, in addition, for compound **21**, the amide homolog of compound **5**. As an example, the binding mode of compounds **5** and **21** is described representing the ester and amide substitutions at position 8 of the [1,2,4]triazolo[1,5-*c*]pyrimidine scaffold.

Formattato: Non Apice / Pedice

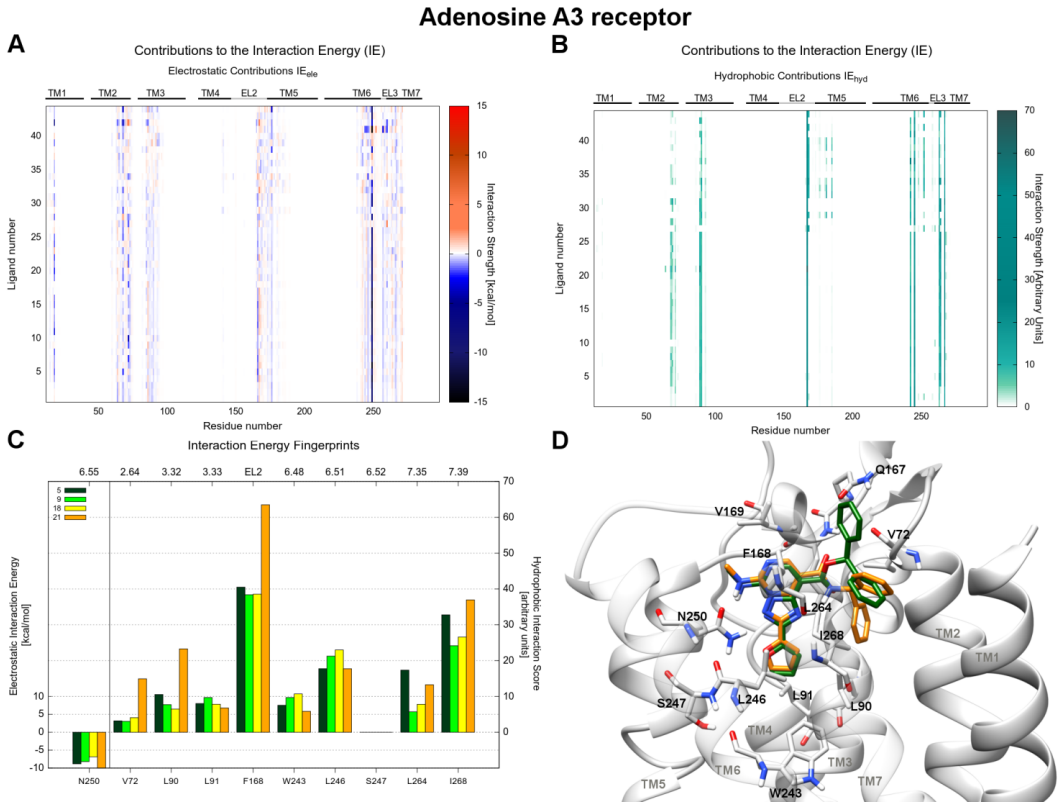

Figure 4. Panel A. Electrostatic Interaction Energy Fingerprints (IEFele) shown as heat map reporting the electrostatic interaction between each compound (y-axis) and each residue (x-axis) of hA_3AR. The strength of the interaction is rendered by a colorimetric scale going from blue to red for negative to positive values. Panel B. Hydrophobic Interaction Energy Fingerprints (IEFhyd) shown as heat map representing the hydrophobic interaction between each compound (y-axis) and each residue (x-axis) of hA_3AR. The strength of the interaction is rendered by a colorimetric scale going from white to dark green for low to high values. Panel C. Histograms representing electrostatic and hydrophobic interactions of few selected hA_3AR residues with compounds **5** (dark green), **9** (light green), **18** (yellow) and **21** (orange). Panel D. Representation of the predicted structure of the complex between hA_3AR (grey) and compounds **5** (green) and **21** (orange).

Concerning the hA_3-AR, the selected poses of compounds **5** and **21** point the furan substituent at position 2 towards the bottom of the binding pocket, the methylamino group at position 5 towards TM6 and the benzhydrylester or benzhydrylamido substituent at position 8 towards TM2 and TM7 (Figure 4, panel D). The ~~triazolopyrimidine~~ TP scaffold is stabilized by a π-π stacking interaction

Formattato: SpazioDopo: 10 pt

with F168 (EL2), and by hydrophobic interactions with L264 (7.35) and I268 (7.39). Residues L90 (3.32), L91 (3.33), W243 (6.48) and L246 (6.51) define a hydrophobic region that accommodates the furan substituent, while V72 (2.64) contributes to the stabilization of the benzhydryl substituent by hydrophobic effect. The compounds are engaged in a double hydrogen bond with N250 (6.55), where the methylamino group at position 5 behaves as donor and the endocyclic nitrogen at position 3 as acceptor. The presence of the double hydrogen bond with an asparagine at position 6.55 is observed also in the other AR subtypes, and explains the loss of affinity of compounds which do not present a hydrogen bond donor at position 5 of the ~~triazolopyrimidine~~ TP scaffold (compounds **50**, **38**, **41**).

With regard to the hA_{2A}-AR (Figure 5, panel D), the ligands are involved in the already described double hydrogen bond with N253 (6.55), the ~~triazolopyrimidine~~ TP scaffold is engaged in a π-π stacking interaction with F168 (EL2) and in a hydrophobic interaction with I274 (7.39), while the interaction with the residue at position 7.35, here M270, is feeble. The furan substituent is positioned in a hydrophobic cleft defined by V84 (3.32), L85 (3.33), W246 (6.48), L249 (6.51), H250 (6.52), while I66 (2.64) is involved in interactions with the benzhydryl group.

A similar binding mode was predicted on hA_1AR (Figure 6, panel D), where the ligands interact through a double hydrogen bond with N254 (6.55) and through a π-π stacking interaction with F168 (EL2). An hydrophobic environment is created also in this case by residues V87 (3.32), L88 (3.33), W247 (6.48), L250 (6.51), close to the furan moiety, and by residues I274 (7.39) and I69 (2.64), surrounding the benzhydryl group. The presence of T270 at position 7.35, which substitutes the L264 encountered in the hA_3 receptor, reduces the hydrophobic interactions between the ligands and the receptor in comparison with hA_3 subtype.

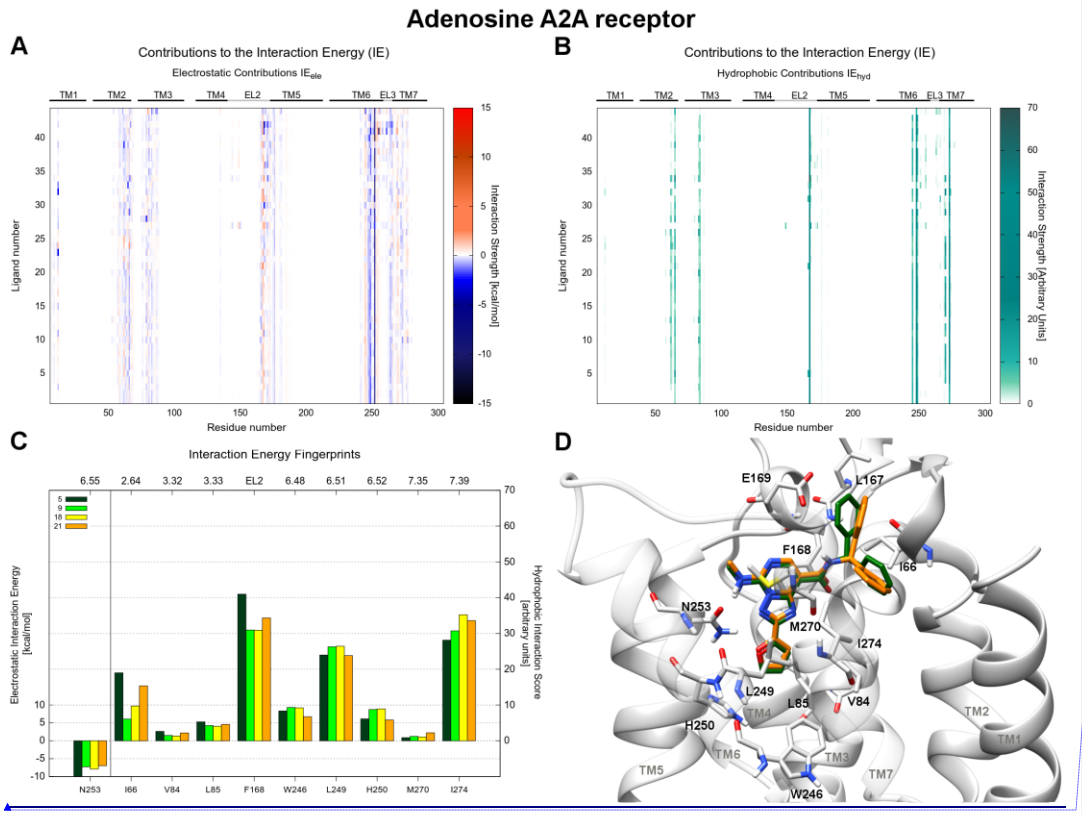

Figure 5. Panel A. Electrostatic Interaction Energy Fingerprints (IEFele) shown as heat map reporting the electrostatic interaction between each compound (y-axis) and each residue (x-axis) of hA_{2A}-AR. The strength of the interaction is rendered by a colorimetric scale going from blue to red for negative to positive values. Panel B. Hydrophobic Interaction Energy Fingerprints (IEFhyd) shown as heat map representing the hydrophobic interaction between each compound (y-axis) and each residue (x-axis) of hA_{2A}–AR. The strength of the interaction is rendered by a colorimetric scale going from white to dark green for low to high values. Panel C. Histograms representing electrostatic and hydrophobic interactions of few selected ~~Ha_{2A}~~ hA_{2A}AR residues with compounds **5** (dark green), **9** (light green), **18** (yellow) and **21** (orange). Panel D. Representation of the predicted structure of the complex between hA_{2A}-AR (grey) and compounds **5** (green) and **21** (orange).

Formattato: Tipo di carattere: 12 pt, Colore carattere: Automatico

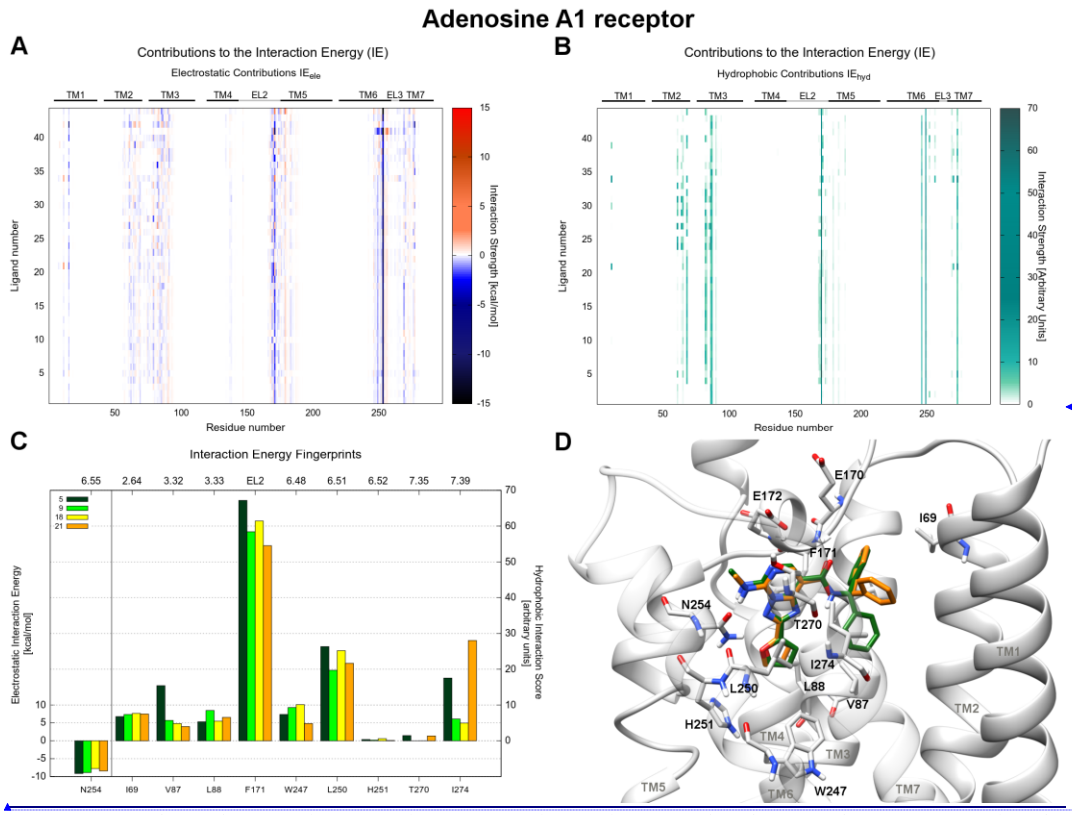

Figure 6. Panel A. Electrostatic Interaction Energy Fingerprints (IEFele) shown as heat map reporting the electrostatic interaction between each compound (y-axis) and each residue (x-axis) of hA_1-AR. The strength of the interaction is rendered by a colorimetric scale going from blue to red for negative to positive values. Panel B. Hydrophobic Interaction Energy Fingerprints (IEFhyd) shown as heat map representing the hydrophobic interaction between each compound (y-axis) and each residue (x-axis) of hA_1-AR. The strength of the interaction is rendered by a colorimetric scale going from white to dark green for low to high values. Panel C. Histograms representing electrostatic and hydrophobic interactions of few selected hA_1-AR residues with compounds **5** (dark green), **9** (light green), **18** (yellow) and **21** (orange). Panel D. Representation of the predicted structure of the complex between hA_1-AR (grey) and compounds **5** (green) and **21** (orange).

In general, the compounds under investigation present a slight selectivity towards hA_3 receptor, which is difficult to be rationalized by molecular docking results, in which a hypothesis on just the static and final situation of the complex binding process is proposed. Considering the dynamic ~~behavior~~behaviour of the receptor, a relevance can be attributed to two residues of EL2 that

Formattato: Tipo di carattere: 12 pt, Colore carattere: Automatico

Formattato: SpazioDopo: 10 pt

differentiates the hA_3 from the other subtype, but which are not directly involved in interactions in the docked poses. The position that in hA_1AR and hA_{2A}AR is occupied by a glutamate (E172 and E169, respectively), in hA_3AR is substituted by V169 (EL2), which can better stabilize the methylamino group in 5. Moreover, E170 of hA_1 and L167 of hA_{2A} are replaced by Q167 on hA_3 receptor, which can play a role in the stabilization of both the ester and amide moiety at position 8, acting as hydrogen bond donor as well as acceptor.

Formattato: Non Apice / Pedice

Conclusions

A novel series of [1,2,4]triazolo[1,5-*c*]pyrimidines variously substituted at the 8 and 5 position (**3-43**) were synthesized as A_3 adenosine receptor antagonists and pharmacologically characterized at the four adenosine receptor subtypes. In all cases, substitution at the 5 position had a detrimental effect in terms of affinity towards hA_3-AR. Instead, substitution at the 8 position of TP with various esters and amides generally led to hA_3–AR antagonists with affinity in the nanomolar range. Unfortunately, selectivity against the other adenosine receptor subtypes was not improved; in fact, obtained compounds displayed similar or worse selectivity profile than reference compound **1**. The only exception was the 4-trifluoromethylbenzylamido derivative **24**, which showed a quite good affinity at the hA_3-AR (K_i= 15.3 nM) accompanied to an optimal selectivity against hA_1, hA_{2A} and hA_{2B} ARs. This ~~behaviour~~behavior is difficult to be rationalized by molecular docking studies, in fact, the ligands bind the three AR subtypes in a similar fashion. In conclusion, despite the goal to obtain potent hA_3–AR antagonists with a [1,2,4]triazolo[1,5-*c*]pyrimidine scaffold was achieved, selectivity against other AR subtypes remains unmet. Future perspectives will be the exploration of the 2 position of the TP scaffold, in order to assess its role in regulation of affinity/selectivity at the four ARs.

Experimental part

Chemistry

General: Reactions were routinely monitored by thin-layer chromatography (TLC) on silica gel (precoated F254 Macherey-Nagel aluminium sheets). Flash chromatography was performed using

Macherey-Nagel 230-400 mesh silica gel. Light petroleum ether refers to the fractions boiling at 40-60 °C. Melting points were determined on a Büchi-Tottoli instrument and are uncorrected. ^{1}H-NMR were determined in $CDCl_3$, DMSO-d_6, or D_2O solutions with a Varian Gemini 200 spectrometer , peaks positions are given in parts per million (δ downfield relative to the central peak of the solvent~~, and J values are given in Hz~~). The following abbreviations were used: s, singlet; bs, broad singlet; d, doublet; dd, double doublet; t, triplet; q, quartet; m, multiplet. Electrospray mass spectra were recorded on an ES_Bruker 4000 Esquire spectrometer, accurate mass spectra were recorded on micrOTOF-Q~~--~~Bruker and compounds were dissolved in methanol.

Procedures for the obtainment of compounds **1,44-49** were previously reported.[16]

General procedure for the synthesis of ester and amide derivatives ***3-~~33~~32***

To 2.45 mmol of carboxylic acid derivatives (**47**) dissolved in 0.7 mL of dry pyridine were added 0.1 mL of phosphorous oxychloride. The mixture was led to -10°C and then was added 39.2 mmol of the appropriate amine or alcohol. The reaction was stirred at room temperature for 16 hours, then was added water and the product extracted with ethylacetate. The organic layer was washed with a $NaHCO_3$ solution, dried and concentrated. The residue was purified by flash chromatography (Ethyl acetate 9 : Light Petroleum 1).

2-Furan-2-yl-5-methylamino-[1,2,4]triazolo[1,5-c]pyrimidine-8-carboxylic acid isopropyl ester (**3**): yield 12%; pale yellow solid; mp 161°C; ^{1}H-NMR (200 MHz, $CDCl_3$) δ 1.41 (6H, d, *J*=6.2 Hz), 3.30 (3H, d, *J*=5.1 Hz), 5.32 (1H, m), 6.58-6.65 (2H, m), 7.38 (1H, d, *J*=4.1 Hz), 7.61 (1H, d, *J*=2.3 Hz), 8.69 (1H, s). HRMS (ESI/Q-TOF) m/z: $[M+H]^+$ Calcd for $C_{14}H_{16}N_5O_3$ 302.1253; Found 302.1254 (Δ=0.0001); $[M+Na]^+$ Calcd for $C_{14}H_{15}N_5NaO_3$ 324.1073, Found 324.1067 (Δ=0.0006).

2-Furan-2-yl-5-methylamino-[1,2,4]triazolo[1,5-c]pyrimidine-8-carboxylic acid benzyl ester (**4**): yield 31%; brown solid; mp 130°C; ^{1}H-NMR (200 MHz, $CDCl_3$) δ 3.31 (3H, d, J=4.1 Hz), 5.47 (2H, s), 6.60-6.76 (2H, m), 7.33-7.40 (5H, m), 7.56-7.63 (2H, m), 8.76 (1H, s). ES-MS m/z: $[M+H]^+$ 350.1, $[M+Na]^+$ 372.1.

Formattato: Colore carattere: Automatico

2-Furan-2-yl-5-methylamino-[1,2,4]triazolo[1,5-c]pyrimidine-8-carboxylic acid benzhydryl ester (**5**): yield 23%; white solid; mp 117°C; ^{1}H-NMR (200 MHz, $CDCl_3$) δ 3.31 (3H, d, *J*=5.4 Hz), 6.61-6.75 (2H, m), 7.16 (1H, s), 7.29-7.40 (8H, m), 7.59-7.63 (4H, m), 8.81 (1H, s). HRMS (ESI/Q-TOF) m/z: $[M+H]^+$ Calcd for $C_{24}H_{20}N_5O_3$ 426.1566; Found 426.1565 (Δ=0.0001); $[M+Na]^+$ Calcd for $C_{24}H_{19}N_5NaO_3$ 448.1386, Found 448.1384 (Δ=0.0002).

2-Furan-2-yl-5-methylamino-[1,2,4]triazolo[1,5-c]pyrimidine-8-carboxylic acid 2-methyl-benzyl ester (**6**): yield 16%; white solid; mp 170°C; ^{1}H-NMR (200 MHz, $CDCl_3$) δ 2.48 (3H, s), 3.30 (3H, d, *J*=5.4 Hz), 5.47 (2H, s), 6.60 (1H, dd, *J*=2.1 Hz, *J*=4.2 Hz), 6.47 (1H, bs), 7.22-7.28 (3H, m), 7.39 (1H, d, *J*=4.2 Hz), 7.62-7.67 (2H, m), 8.74 (1H, s). HRMS (ESI/Q-TOF) m/z: $[M+H]^+$ Calcd for $C_{19}H_{18}N_5O_3$ 364.1410; Found 364.1415 (Δ=0.0005); $[M+Na]^+$ Calcd for $C_{19}H_{17}N_5NaO_3$ 386.1229, Found 386.1229 (Δ=0).

2-Furan-2-yl-5-methylamino-[1,2,4]triazolo[1,5-c]pyrimidine-8-carboxylic acid 3-methyl-benzyl ester (**7**): yield 13%; white solid; mp 170°C; ^{1}H-NMR (200 MHz, $CDCl_3$) δ 2.38 (3H, s), 3.30 (3H, d, *J*=5.4 Hz), 5.43 (2H, s), 6.59 (1H, dd, *J*=2.1 Hz, *J*=4.2 Hz), 6.67 (1H, bs), 7.13-7.17 (1H, m), 7.24-7.38 (5H, m), 7.61 (1H, d, *J*=2.1 Hz), 8.75 (1H, s). HRMS (ESI/Q-TOF) m/z: $[M+H]^+$ Calcd for $C_{19}H_{18}N_5O_3$ 364.1410; Found 364.1411 (Δ=0.0001); $[M+Na]^+$ Calcd for $C_{19}H_{17}N_5NaO_3$ 386.1229, Found 386.1229 (Δ=0).

2-Furan-2-yl-5-methylamino-[1,2,4]triazolo[1,5-c]pyrimidine-8-carboxylic acid 4-methyl-benzyl ester (**8**): yield 23%; white solid; mp 202°C; ^{1}H-NMR (200 MHz, $CDCl_3$) δ 2.36 (3H, s), 3.29 (3H, d, *J*=5.4 Hz), 5.42 (2H, s), 6.59-6.64 (2H, m), 7.20 (2H, d, *J*=8.3 Hz), 7.37 (1H, d, *J*=4.1 Hz), 7.45 (2H, d, *J*=8.3 Hz), 7.62 (1H, d, *J*=2.1 Hz), 8.73 (1H, s). HRMS (ESI/Q-TOF) m/z: $[M+H]^+$ Calcd for $C_{19}H_{18}N_5O_3$ 364.1410; Found 364.1403 (Δ=0.0007); $[M+Na]^+$ Calcd for $C_{19}H_{17}N_5NaO_3$ 386.1229, Found 386.1221 (Δ=0.0008).

2-Furan-2-yl-5-methylamino-[1,2,4]triazolo[1,5-c]pyrimidine-8-carboxylic acid 2-methoxy-benzyl ester (**9**): yield 19%; white solid; mp 181°C; ^{1}H-NMR (200 MHz, $CDCl_3$) δ 3.30 (3H, d, *J*=5.4 Hz), 3.87 (3H, s), 5.51 (2H, s), 6.58-6.63 (2H, m), 6.89-7.06 (2H, m), 7.37 (1H, d, *J*=4.1 Hz), 7.62 (1H,

d, *J*=2.3 Hz), 7.76 (1H, d, *J*=8.3 Hz), 8.76 (1H, s). HRMS (ESI/Q-TOF) m/z: $[M+H]^+$ Calcd for $C_{19}H_{18}N_5O_4$ 380.1359; Found 380.1355 (Δ=0.0004); $[M+Na]^+$ Calcd for $C_{19}H_{17}N_5NaO_4$ 402.1178, Found 402.1174 (Δ=0.0004).

2-Furan-2-yl-5-methylamino-[1,2,4]triazolo[1,5-c]pyrimidine-8-carboxylic acid 3-methoxy-benzyl ester (**10**): yield 13%; white solid; mp 156°C; ^{1}H-NMR (200 MHz, $CDCl_3$) δ 3.30 (3H, d, *J*=5.4 Hz), 3.83 (3H, s), 5.45 (2H, s), 6.59 (1H, dd, *J*=2.1 Hz, *J*=4.3 Hz), 6.70 (1H, bs), 6.87 (1H, dd, *J*=1.6 Hz, *J*=8.3 Hz), 7.11-7.14 (1H, m), 7.20 (1H, m), 7.31-7.35 (1H, m), 7.41 (1H, d, *J*=4.3 Hz), 7.61 (1H, d, *J*=2.1 Hz), 8.76 (1H, s). HRMS (ESI/Q-TOF) m/z: $[M+H]^+$ Calcd for $C_{19}H_{18}N_5O_4$ 380.1359; Found 380.1354 (Δ=0.0005); $[M+Na]^+$ Calcd for $C_{19}H_{17}N_5NaO_4$ 402.1178, Found 402.1171 (Δ=0.0007).

2-Furan-2-yl-5-methylamino-[1,2,4]triazolo[1,5-c]pyrimidine-8-carboxylic acid 4-methoxy-benzyl ester (**11**): yield 23%; white solid; mp 189°C; ^{1}H-NMR (200 MHz, $CDCl_3$) δ 3.29 (3H, d, *J*=5.4 Hz), 3.81 (3H, s), 5.40 (2H, s), 6.60 (1H, dd, *J*=2.1 Hz, *J*=4.3 Hz), 6.70 (1H, bs), 6.91 (2H, dd, *J*=2.1 Hz, *J*=7.2 Hz), 7.36 (1H, d, *J*=4.3 Hz) 7.47 (2H, dd, *J*=2.1 Hz, *J*=7.2 Hz), 7.61 (1H, d, *J*=2).1 Hz, 8.72 (1H, s). HRMS (ESI/Q-TOF) m/z: $[M+H]^+$ Calcd for $C_{19}H_{18}N_5O_4$ 380.1359; Found 380.1364 (Δ=0.0005); $[M+Na]^+$ Calcd for $C_{19}H_{17}N_5NaO_4$ 402.1178, Found 402.1182 (Δ=0.0004).

2-Furan-2-yl-5-methylamino-[1,2,4]triazolo[1,5-c]pyrimidine-8-carboxylic acid 2-chloro-benzyl ester (**12**): yield 29%; white solid; mp 205°C; ^{1}H-NMR (200 MHz, $CDCl_3$) δ 3.29 (3H, d, *J*=5.4 Hz), 5.56 (2H, s), 6.60 (1H, dd, *J*=2.1 Hz, *J*=4.3 Hz), 6.69 (1H, d, *J*=5.4 Hz), 7.28-7.52 (4H, m), 7.62 (1H, d, *J*=2.1 Hz), 7.90 (1H, dd, *J*=2.1 Hz, *J*=7.3 Hz), 8.78 (1H, s). HRMS (ESI/Q-TOF) m/z: $[M+H]^+$ Calcd for $C_{18}H_{15}ClN_5O_3$ 384.0863 and 386.0834; Found 384.0871 (Δ=0.0008) and 386.0850 (Δ=0.0016); $[M+Na]^+$ Calcd for $C_{18}H_{14}ClN_5NaO_3$ 406.0683 and ~~406~~408.0653, Found 406.0688 (Δ=0.0005) and 408.0668 (Δ=0.~~0011~~0015).

2-Furan-2-yl-5-methylamino-[1,2,4]triazolo[1,5-c]pyrimidine-8-carboxylic acid 3-chloro-benzyl ester (**13**): yield 32%; white solid; mp 195°C; ^{1}H-NMR (200 MHz, $CDCl_3$) δ 3.31 (3H, d, *J*=5.4 Hz), 5.44 (2H, s), 6.60 (1H, dd, *J*=2.1 Hz, *J*=4.3 Hz), 6.70 (1H, d, *J*=5.4 Hz), 7.30-7.33 (2H, m),

7.41-7.42 (2H, m), 7.63 (1H, d, *J*=1.2 Hz), 7.68 (1H, d, *J*=2.1 Hz), 8.77 (1H, s). HRMS (ESI/Q-TOF) m/z: $[M+H]^+$ Calcd for $C_{18}H_{15}ClN_5O_3$ 384.0863 and 386.0834; Found 384.0867 (Δ=0.0004) and 386.0857 (Δ=0.0023); $[M+Na]^+$ Calcd for $C_{18}H_{14}ClN_5NaO_3$ 406.0683 and ~~406~~408.0653, Found 406.0680 (Δ=0.0003) and 408.0672 (Δ=0.0019).

2-Furan-2-yl-5-methylamino-[1,2,4]triazolo[1,5-c]pyrimidine-8-carboxylic acid 4-chloro-benzyl ester (**14**): yield 32%; white solid; mp 205°C; ^{1}H-NMR (200 MHz, $CDCl_3$) δ 3.30 (3H, d, *J*=5.4 Hz), 5.43 (2H, s), 6.62 (1H, dd, *J*=2.1 Hz, *J*=4.3 Hz), 6.69 (1H, d, *J*=5.4 Hz), 7.32-7.40 (3H, m), 7.53 (2H, d, *J*=8.3 Hz), 7.62 (1H, d, *J*=2.1 Hz), 8.75 (1H, s). HRMS (ESI/Q-TOF) m/z: $[M+H]^+$ Calcd for $C_{18}H_{15}ClN_5O_3$ 384.0863 and 386.0834; Found 384.0869 (Δ=0.0006) and 386.0850 (Δ=0.0016); $[M+Na]^+$ Calcd for $C_{18}H_{14}ClN_5NaO_3$ 406.0683 and ~~406~~408.0653, Found 406.0685 (Δ=0.0002) and 408.0658 (Δ=0.0005).

2-Furan-2-yl-5-methylamino-[1,2,4]triazolo[1,5-c]pyrimidine-8-carboxylic acid 2-bromo-benzyl ester (**15**): yield 17%; white solid; mp 223°C; ^{1}H-NMR (200 MHz, $CDCl_3$) δ 3.31 (3H, d, *J*=5.4 Hz), 5.53 (2H, s), 6.60 (1H, dd, *J*=2.1 Hz, *J*=4.3 Hz), 6.68 (1H, bs), 7.19 (1H, d, *J*=6.2 Hz), 7.35-7.42 (2H, m), 7.58-7.63 (2H, m), 7.91 (1H, d, *J*=8.3 Hz), 8.80 (1H, s). HRMS (ESI/Q-TOF) m/z: $[M+H]^+$ Calcd for $C_{18}H_{15}BrN_5O_3$ 428.0358 and 430.0338; Found 428.0368 (Δ=0.~~000~~0010) and 430.~~0344~~ 0345 (Δ=0.~~0006~~0007); $[M+Na]^+$ Calcd for $C_{18}H_{14}BrN_5NaO_3$ 450.0178 and 452.0157, Found 450.~~0174~~ 0175 (Δ=0.~~0004~~0003) and 452.~~0166~~ 0164 (Δ=0.~~0009~~0007).

2-Furan-2-yl-5-methylamino-[1,2,4]triazolo[1,5-c]pyrimidine-8-carboxylic acid 3-fluoro-benzyl ester (**16**): yield 4.4%; white solid; mp 193°C; ^{1}H-NMR (200 MHz, $CDCl_3$) δ 3.30 (3H, d, *J*=5.4 Hz), 5.46 (2H, s), 6.61 (1H, dd, *J*=2.1 Hz, *J*=4.3 Hz), 6.70 (1H, d, *J*=5.4 Hz), 6.99-7.07 (1H, m), 7.31-7.41 (3H, m), 7.53 (1H, d, *J*=10.6 Hz), 7.63 (1H, d, *J*=2.1 Hz), 8.77 (1H, s). HRMS (ESI/Q-TOF) m/z: $[M+Na]^+$ Calcd for $C_{18}H_{14}FN_5NaO_3$ 390.0978 and 391.1012, Found 390.0983 (Δ=0.0005) and 391.1013 (Δ=0.0001).

2-Furan-2-yl-5-methylamino-[1,2,4]triazolo[1,5-c]pyrimidine-8-carboxylic acid 4-fluoro-benzyl ester (**17**): yield 16%; white solid; mp 181°C; ^{1}H-NMR (200 MHz, $CDCl_3$) δ 3.30 (3H, d, *J*=5.4

Hz), 5.43 (2H, s), 6.61 (1H, dd, *J*=2,.1 Hz *J*=4.3 Hz), 6.68 (1H, bs), 7.03-7.12 (2H, m), 7.34 (1H, d, *J*=4.3 Hz), 7.53-7.63 (3H, m), 8.74 (1H, s). HRMS (ESI/Q-TOF) m/z: $[M+Na]^+$ Calcd for $C_{18}H_{14}FN_5NaO_3$ 390.0978 and 391.1012, Found 390.0985 (Δ=0.0007) and 391.1013 (Δ=0.0001).

2-Furan-2-yl-5-methylamino-[1,2,4]triazolo[1,5-c]pyrimidine-8-carboxylic acid 4-ethyl-benzyl ester (**18**): yield 16%; white solid; mp 175°C; ^{1}H-NMR (200 MHz, $CDCl_3$) δ 1.24 (3H, t, *J*=8.2 Hz), 2.66 (2H, q, *J*=8.2 Hz), 3.29 (3H, d, *J*=5.4 Hz), 5.43 (2H, s), 6.59-6.65 (2H, m), 7.20-7.24 (2H, m), 7.36 (1H, d, *J*=4.3 Hz), 7.47 (2H, d, *J*=8.2 Hz), 7.62 (1H, d, *J*=2.1 Hz), 8.74 (1H, bs). ^{13}C NMR (101 MHz, $CDCl_3$) δ 163.31, 158.03, 152.22, 151.86, 148.64, 145.71, 144.80, 144.41, 133.46, 128.35, 128.15, 113.91, 112.17, 104.74, 66.71, 28.78, 28.11, 15.76. HRMS (ESI/Q-TOF) m/z: $[M+H]^+$ Calcd for $C_{20}H_{20}N_5O_3$ 378.1566; Found 378.1574 (Δ=0.0008); $[M+Na]^+$ Calcd for $C_{20}H_{19}N_5NaO_3$ 400.1386, Found 400.1389 (Δ=0.0003).

2-Furan-2-yl-5-methylamino-[1,2,4]triazolo[1,5-c]pyrimidine-8-carboxylic acid 1-methyl-2-phenyl-ethyl ester (**19**): yield 18%; brown sticky foam; ^{1}H-NMR (200 MHz, $CDCl_3$) δ 1.39 (3H, d, *J*=6.3 Hz), 2.97-3.15 (2H, m), 3.28 (3H, s), 5.42-5.48 (1H, m), 6.58 (1H, dd, *J*=2.1 Hz, *J*=4.3 Hz), 6.76 (1H, bs), 7.19-7.39 (6H, m), 7.61 (1H, d, *J*=2.1 Hz), 8.65 (1H, s). ES-MS m/z: $[M+H]^+$ 400.1.

2-Furan-2-yl-5-methylamino-[1,2,4]triazolo[1,5-c]pyrimidine-8-carboxylic acid benzylamide (**20**): yield 16%; white solid; mp 246°C; ^{1}H-NMR (200 MHz, $CDCl_3$) δ 3.30 (3H, d, *J*=5.4 Hz), 4.77 (2H, d, *J*=6.2 Hz), 6.49 (1H, bs), 6.59 (1H, dd, *J*=2.1 Hz, *J*=4.3 Hz), 7.16 (1H, d, *J*=4.3 Hz), 7.32-7.46 (5H, m), 7.62 (1H, d, *J*=2.1 Hz), 8.86 (1H, s). HRMS (ESI/Q-TOF) m/z: $[M+Na]^+$ Calcd for $C_{18}H_{16}N_6NaO_2$ 371.1232, Found 371.1236 (Δ=0.0004).

Formattato: Tipo di carattere: Corsivo

2-Furan-2-yl-5-methylamino-[1,2,4]triazolo[1,5-c]pyrimidine-8-carboxylic acid benzhydryl-amide (**21**): yield 42%; pale yellow solid solid; mp 199°C; ^{1}H-NMR (200 MHz, $CDCl_3$) δ 3.32 (3H, d, *J*=5.4 Hz), 6.50-6.53 (2H, m), 6.63 (1H, dd, *J*=2.1 Hz, *J*=4.3 Hz), 7.15 (1H, d, *J*=4.3 Hz),7.21-7.46 (10H, m), 7.66 (1H, d, *J*=2.1 Hz), 8.85 (1H, s), 9.72 (1H, d, *J*=8.2 Hz). HRMS (ESI/Q-TOF) m/z: $[M+H]^+$ Calcd for $C_{24}H_{21}N_6O_2$ 425.1726, Found 425.1722 (Δ=0.0004); $[M+Na]^+$ Calcd for $C_{24}H_{20}N_6NaO_2$ 447.1545, Found 447.1541 (Δ=0.0004).

2-Furan-2-yl-5-methylamino-[1,2,4]triazolo[1,5-c]pyrimidine-8-carboxylic acid 4-methyl-benzylamide (**22**): yield 11%; white solid; mp 236°C; ^{1}H-NMR (200 MHz, $CDCl_3$) δ 2.35 (3H, s), 3.30 (3H, d, *J*=5.4 Hz), 4.72 (2H, d, *J*=5.4 Hz), 6.43 (1H, bs), 6.59 (1H, dd, *J*=2.1 Hz, *J*=4.3 Hz), 7.16-7.35 (5H, m), 7.62 (1H, d, *J*=2.1 Hz), 8.66 (1H, s), 9.03 (1H, bs). HRMS (ESI/Q-TOF) m/z: $[M+H]^+$ Calcd for $C_{19}H_{19}N_6O_2$ 363.1569, Found 363.1564 (Δ=0.0005); $[M+Na]^+$ Calcd for $C_{19}H_{18}N_6NaO_2$ 385.1389, Found 385.1382 (Δ=0.0007).

2-Furan-2-yl-5-methylamino-[1,2,4]triazolo[1,5-c]pyrimidine-8-carboxylic acid 4-methoxy-benzylamide (**23**): yield 20%; pale yellow solid; mp 232°C; ^{1}H-NMR (200 MHz, $CDCl_3$) δ 3.29 (3H, d, *J*=5.4 Hz), 3.80 (3H, s), 4.69 (2H, d, *J*=5.4 Hz), 6.48 (1H, bs), 6.58 (1H, dd, *J*=2.1 Hz, *J*=4.3 Hz), 6.90 (2H, dd, *J*=2.1 Hz, *J*=7.2 Hz), 7.15 (1H, d, *J*=4.3 Hz), 7.37 (2H, dd, *J*=2.1 Hz, *J*=7.2 Hz), 7.62 (1H, d, *J*=2.1 Hz), 8.85 (1H, s), 8.99 (1H, bs). HRMS (ESI/Q-TOF) m/z: $[M+H]^+$ Calcd for $C_{19}H_{19}N_6O_3$ 379.1519, Found 379.1522 (Δ=0.0003); $[M+Na]^+$ Calcd for $C_{19}H_{18}N_6NaO_3$ 401.1338, Found 401.1341 (Δ=0.0003).

2-Furan-2-yl-5-methylamino-[1,2,4]triazolo[1,5-c]pyrimidine-8-carboxylic acid 4-trifluoromethyl-benzylamide (**24**): yield 18%; orange solid; mp 249°C; ^{1}H-NMR (200 MHz, $CDCl_3$) δ 3.31 (3H, d, *J*=5.4 Hz), 4.82 (2H, d, *J*=5.4 Hz), 6.52 (1H, bs), 6.60 (1H, dd, *J*=2.1 Hz, *J*=4.3 Hz), 7.17 (1H, d, *J*=4.3 Hz), 7.52-7.64 (5H, m), 8.86 (1H, s), 9.13 (1H, bs). HRMS (ESI/Q-TOF) m/z: $[M+H]^+$ Calcd for $C_{19}H_{16}F_3N_6O_2$ 417.1287, Found 417.1315 (Δ=0.0028).

2-Furan-2-yl-5-methylamino-[1,2,4]triazolo[1,5-c]pyrimidine-8-carboxylic acid 4-chloro-benzylamide (**25**): yield 13%; pale brown solid; mp 225°C; ^{1}H-NMR (200 MHz, $CDCl_3$) δ 3.30 (3H, d, *J*=5.4 Hz), 4.72 (2H, d, *J*=5.4 Hz), 6.52 (1H, bs), 6.60 (1H, dd, *J*=2.1 Hz, *J*=4.3 Hz), 7.17 (1H, d, *J*=4.3 Hz), 7.29-7.35 (4H, m), 7.63 (1H, d, *J*=2.1 Hz), 8.85 (1H, s), 9.06 (1H, bs). HRMS (ESI/Q-TOF) m/z: $[M+Na]^+$ Calcd for $C_{18}H_{15}ClN_6NaO_2$ 405.0843 and 407.0813, Found 405.0847 (Δ=0.0004) and 407.0820 (Δ=0.0007).

2-Furan-2-yl-5-methylamino-[1,2,4]triazolo[1,5-c]pyrimidine-8-carboxylic acid 4-fluoro-benzylamide (**26**): yield 26%; white solid; mp 225°C; ^{1}H-NMR (200 MHz, $CDCl_3$) δ 3.30 (3H, d,

J=5.4 Hz), 4.72 (2H, d, *J*=5.4 Hz), 6.51 (1H, bs), 6.59 (1H, dd, *J*=2.1 Hz, *J*=4.3 Hz), 7.00-7.09 (2H, m), 7.15 (1H, d, *J*=4.3 Hz), 7.36-7.43 (2H, m), 7.63 (1H, d, *J*=2.1 Hz), 8.85 (1H, s), 9.05 (1H, bs). HRMS (ESI/Q-TOF) m/z: $[M+H]^+$ Calcd for $C_{18}H_{16}FN_6O_2$ 367.1319, Found 367.1310 (Δ=0.~~0001~~0009); $[M+Na]^+$ Calcd for $C_{18}H_{15}FN_6NaO_2$ 389.1138, Found 389.1131 (Δ=0.0007).

2-Furan-2-yl-5-methylamino-[1,2,4]triazolo[1,5-c]pyrimidine-8-carboxylic acid (biphenyl-4-ylmethyl)-amide (**27**): yield 5.5%; pale yellow solid; mp>250°C; ^{1}H-NMR (200 MHz, DMSO-d_6) δ 3.01 (3H, d, *J*=5.4 Hz), 4.70 (2H, d, *J*=5.4 Hz), 6.75 (1H, dd, *J*=2.1 Hz, *J*=4.3 Hz), 7.32 (1H, d, *J*=4.3 Hz), 7.38-7.50 (5H, m), 6.66 (4H, d, *J*=8.2 Hz), 7.98 (1H, d, *J*=2.1 Hz), 8.58 (1H, s), 8.92 (1H, bs), 9.10 (1H, bs). HRMS (ESI/Q-TOF) m/z: $[M+H]^+$ Calcd for $C_{24}H_{21}N_6O_2$ 425.1726, Found 425.1726 (Δ=0); $[M+Na]^+$ Calcd for $C_{24}H_{20}N_6NaO_2$ 447.1545, Found 447.1546 (Δ=0.0001).

2-Furan-2-yl-5-methylamino-[1,2,4]triazolo[1,5-c]pyrimidine-8-carboxylic acid 3,4-dimethoxy-benzylamide (**28**): yield 23%; pale yellow solid; mp 190°C; ^{1}H-NMR (200 MHz, $CDCl_3$) δ 3.30 (3H, d, *J*=5.4 Hz), 3.88 (6H, s), 4.70 (2H, d, *J*=5.4 Hz), 6.51 (1H, bs), 6.58 (1H, dd, *J*=2.1 Hz, *J*=4.3 Hz), 6.88 (1H, m), 7.33-7.40 (5H, m), 7.56-7.63 (2H, m), 8.76 (1H, s). HRMS (ESI/Q-TOF) m/z: $[M+H]^+$ Calcd for $C_{20}H_{21}N_6O_4$ 409.1624, Found 409.1630 (Δ=0.0006); $[M+Na]^+$ Calcd for $C_{20}H_{20}N_6NaO_4$ 431.1444, Found 431.1443 (Δ=0.0001).

2-Furan-2-yl-5-methylamino-[1,2,4]triazolo[1,5-c]pyrimidine-8-carboxylic acid phenethyl-amide (**29**): yield 45%; pale yellow solid solid; mp 204°C; ^{1}H-NMR (200 MHz, $CDCl_3$) δ 3.00 (2H., t, *J*=7.2 Hz), 3.29 (3H, d, *J*=5.4 Hz), 3.83 (2H, q, *J*=7.2 Hz), 6.49 (1H, bs), 6.60 (1H, dd, *J*=2.1 Hz, *J*=4.3 Hz), 7.09 (1H, d, *J*=4.3 Hz), 7.27-7.34 (5H, m), 7.64 (1H, d, *J*=2.1 Hz), 8.69 (1H, bs), 8.82 (1H, s). HRMS (ESI/Q-TOF) m/z: $[M+H]^+$ Calcd for $C_{19}H_{20}N_6O_2$ 363.1570, Found 363.1566 (Δ=0.0004); $[M+Na]^+$ Calcd for $C_{19}H_{18}N_6NaO_2$ 385.1389, Found 385.1388 (Δ=0.0001).

2-Furan-2-yl-5-methylamino-[1,2,4]triazolo[1,5-c]pyrimidine-8-carboxylic acid [2-(3,4-dimethoxy-phenyl)-ethyl]-amide (**30**): yield 25%; pale yellow solid solid; mp 211°C; ^{1}H-NMR (200 MHz, $CDCl_3$) δ 2.94 (2H, t, *J*=7.2 Hz), 3.29 (3H, d, *J*=5.4 Hz), 3.74-3.86 (8H, m), 6.50 (1H, bs), 6.60 (1H, dd, *J*=2.1 Hz, *J*=4.3 Hz), 6.83-6.88 (3H, m), 7.07 (1H, d, *J*=4.3 Hz), 7.64 (1H, d, *J*=2.1 Hz),

Formattato: Tipo di carattere: Corsivo

8.70 (1H, bs), 8.83 (1H, s). HRMS (ESI/Q-TOF) m/z: $[M+H]^+$ Calcd for $C_{21}H_{23}N_6O_4$ 423.1781; Found 423.1782 (Δ=0.0001); $[M+Na]^+$ Calcd for $C_{21}H_{22}N_6NaO_4$ 445.1600, Found 445.1605 (Δ=0.0005).

2-Furan-2-yl-5-methylamino-[1,2,4]triazolo[1,5-c]pyrimidine-8-carboxylic acid (1,1-dimethyl-2-phenyl-ethyl)-amide (**31**): yield 40%; white solid solid; mp 172°C; ^{1}H-NMR (200 MHz, $CDCl_3$) δ 1.52 (6H, s), 3.23 (2H, s), 3.29 (3H, d, *J*=5.4 Hz), 6.44 (1H, bs), 6.57 (1H, dd, *J*=2.1 Hz, *J*=4.3 Hz), 7.12 (1H, d, *J*=4.3 Hz), 7.18-7.27 (5H, m), 7.62 (1H, d, *J*=2.1 Hz), 8.58 (1H, bs), 8.82 (1H, s). ^{13}C NMR (101 MHz, $CDCl_3$) δ 161.87, 156.32, 151.60, 150.22, 147.82, 145.38, 145.00, 138.14, 130.82, 128.00, 126.34, 113.45, 112.11, 107.27, 54.85, 46.10, 28.11, 27.20. HRMS (ESI/Q-TOF) m/z: $[M+H]^+$ Calcd for $C_{21}H_{23}N_6O_2$ 391.1883; Found 391.1886 (Δ=0.0003); $[M+Na]^+$ Calcd for $C_{21}H_{22}N_6NaO_2$ 413.1702, Found 413.1703 (Δ=0.0001).

2-Furan-2-yl-5-methylamino-[1,2,4]triazolo[1,5-c]pyrimidine-8-carboxylic acid (2-phenoxy-ethyl)-amide (**32**): yield 34%; white solid solid; mp 198°C; ^{1}H-NMR (200 MHz, $CDCl_3$) δ 3.29 (3H, d, *J*=5.4 Hz), 3.96 (2H, q, *J*=5.2 Hz), 4.23 (2H, q, *J*=5.2 Hz) 6.50 (1H, d, *J*=5.4 Hz), 6.58 (1H, dd, *J*=2.1 Hz, *J*=4.3 Hz), 6.70-7.03 (3H, m), 7.15 (1H, d, *J*=4.3 Hz), 7.30-7.34 (2H, m), 7.63 (1H, d, *J*=2.1 Hz), 8.83 (1H, bs), 9.13 (1H, s). HRMS (ESI/Q-TOF) m/z: $[M+H]^+$ Calcd for $C_{19}H_{19}N_6O_3$ 379.1519; Found 379.1530 (Δ=0.0011); $[M+Na]^+$ Calcd for $C_{19}H_{18}N_6NaO_3$ 401.1338, Found 401.1347 (Δ=0.0009).

Procedure for the synthesis of 2-furan-2-yl-5-methylamino-[1,2,4]triazolo[1,5-c]pyrimidine-8-carboxylic acid N'-phenyl-hydrazide (**33**).

150 mg of compound **47** (0.58 mmol) were dissolved in 10 mL of ethanol, then 333 mg of *N*-(3-dimethylaminopropyl)-*N'*-ethylcarbodiimide hydrochloride (1.74 mmol), 235 mg of 1-hydroxybenzotriazole hydrate (1.74 mmol) and 68 μL of phenylhydrazine (0.70 mmol) were added. The mixture was stirred at room temperature overnight. Then, ethanol was removed under reduced pressure and 30 mL of water were added to the residue. The product was extracted three times with

10 mL of ethylacetate. The organic layers were combined, dried over anhydrous sodium sulfate and concentrated. The residue was purified by flash chromatography (from Light Petroleum 7 : Ethyl acetate 3 to Light Petroleum 3 : Ethyl acetate 7) to afford 79 mg of a pale yellow solid (yield 39%). Mp>220°C; ^{1}H-NMR (200 MHz, $CDCl_3$) δ 3.30 (3H, d, *J*=5.4 Hz), 6.60-6.63 (2H, m), 6.91-7.00 (3H, m), 7.21-7.29 (4H, m), 7.65 (1H, d, *J*=2.1 Hz), 8.82 (1H, s), 10.03 (1H, bs). ES-MS m/z: $[M+H]^+$ 350.2, $[M+Na]^+$ 372.2, $[M+K]^+$ 388.1.

Synthesis of 5-(3,4-Dimethoxy-benzylamino)-2-furan-2-yl-[1,2,4]triazolo[1,5-c]pyrimidine-8-carboxylic acid benzhydryl-amide (**34**).

For the synthesis of compound **34** was applied the same procedure reported for derivatives **3-~~33~~ 32** but using derivative **49** as carboxylic acid derivative and benzhydrylamine as amine. Yield 63%; pale brown solid; mp 170°C; ^{1}H-NMR (200 MHz, $CDCl_3$) δ 3.85 (6H, s), 4.82 (2H, d, *J*=6.2 Hz), 6.48 (1H, d, *J*=6.2 Hz), 6.60 (1H, dd, *J*=2.1 Hz, *J*=4.3 Hz), 6.74 (1H, bs), 6.82-6.98 (3H, m), 7.14 (1H, d, J=4.3 Hz), 7.32-7.46 (10H, m), 7.62 (1H, d, *J*=2.1 Hz), 8.88 (1H, s), 9.68 (1H, d, *J*=6.4 Hz). ES-MS (negative mode) m/z: $[M-H]^-$ 559.2.

*General procedure for nucleophilic substitution with amino compounds (compounds **35-39**)*

To 100 mg (0.33 mmol) of compound **46** dissolved in ethanol was added the appropriate amine (0.99 mmol to 1.98 mmol). The mixture was heated in a sealed tube at 120°C for three hours. The solvent was then removed and the residue was purified by flash chromatography (from Light petroleum 7 : Ethyl acetate 3 to Ethyl acetate). ~~Sometimes ethyl 5-ethoxy-2-(furan-2-yl)-[1,2,4]triazolo[1,5-*c*]pyrimidine-8-carboxylate (**50**) was obtained as by-product. Derivative **50** was isolated and characterized (see below for chemical characterization).~~

*ethyl 2-(5-((2-ethoxy-2-oxoethyl)amino)-2-(furan-2-yl)-[1,2,4]triazolo[1,5-c]pyrimidine-8-carboxamido)acetate (**35**)*: reaction was performed using 138 mg of glycine ethyl ester hydrochloride (0.990 mmol) and 138 µL of TEA (0.99 mmol) leading to concomitant substitution at the 5 position and amidation at the 8 position of [1,2,4]triazolo[1,5-*c*]pyrimidine; yield 55%; pale

yellow solid; mp 182°C; ^{1}H-NMR (200 MHz, $CDCl_3$) δ 1.28 (3H, t, *J*=7.2 Hz), 1.44 (3H, t, *J*=7.2 Hz), 4.12 (2H, d, *J*=5.4 Hz), 4.22 (2H, q, *J*=7.2 Hz), 4.47 (4H, m), 6.59 (1H, dd, *J*=2.1 Hz, *J*=4.3 Hz), 6.76 (1H, bs), 7.35 (2H, m), 7.62 (1H, d, *J*=2.1 Hz), 8.65 (1H, s). HRMS (ESI/Q-TOF) m/z: $[M+H]^+$ Calcd for $C_{18}H_{21}N_6O_6$ 417.1523; Found 417.1521 (Δ=0.0002); $[M+Na]^+$ Calcd for $C_{18}H_{20}N_6NaO_6$ 439.1342, Found 439.1341 (Δ=0.0001).

Ethyl 2-(furan-2-yl)-5-(2-phenylhydrazinyl)-[1,2,4]triazolo[1,5-c]pyrimidine-8-carboxylate (***36***): reaction was performed using 97 µL of phenylhydrazine (1.32 mmol); yield 71%; brown solid; mp 141-155 °C; ^{1}H-NMR (200 MHz, $CDCl_3$) δ 1.42 (3H, t, *J*=7.2 Hz), 4.46 (2H, q, *J*=7.2 Hz), 6.62 (1H, dd, *J*=2.1 Hz, *J*=4.3 Hz), 6.95-6.99 (3H, m), 7.22-7.28 (4H, m), 7.43 (1H, d, *J*=3.2 Hz), 7.65 (1H, d, *J*=2.1 Hz), 8.66 (1H, s). ES-MS m/z: $[M+H]^+$ 365.1, $[M+Na]^+$ 387.1.

5-(2-tert-Butoxycarbonylamino-ethylamino)-2-furan-2-yl-[1,2,4]triazolo[1,5-c]pyrimidine-8-carboxylic acid ethyl ester (**37**): reaction was performed using 159 mg of mono-Boc-ethylendiamine (0.99 mmol); yield 45%; pale yellow solid; mp 170°C; ^{1}H-NMR (200 MHz, $CDCl_3$) δ 1.43-1.53 (12H, m), 3.52 (2H, bs), 3.83 (2H, bs), 4.47 (2H, q, *J*=7.2 Hz), 4.92 (1H, bs), 6.59 (1H, dd, *J*=2.1 Hz, *J*=4.3 Hz), 7.14 (1H, bs), 7.37 (1H, d, *J*=4.3 Hz), 7.62 (1H, d, *J*=2.1 Hz), 8.68 (1H, s). ES-MS m/z: $[M+Na]^+$ 439.2.

Ethyl 5-(4-(tert-butoxycarbonyl)piperazin-1-yl)-2-(furan-2-yl)-[1,2,4]triazolo[1,5-c]pyrimidine-8-carboxylate (***38***): reaction was performed using 245 mg of N-Boc-pyperazine (1.32 mmol); yield 28%; white solid; mp 170°C; ^{1}H-NMR (200 MHz, $CDCl_3$) δ 1.40-1.50 (12H, m), 3.63-3.68 (4H, m), 4.32-4.34 (4H, m), 4.47 (2H, q, *J*=7), 6.57 (1H, dd, *J*=2, *J*=4), 7.34 (1H, d, *J*=4), 7.61 (1H, d, *J*=2), 8.64 (1H, s). HRMS (ESI/Q-TOF) m/z: $[M+H]^+$ Calcd for $C_{21}H_{27}N_6O_5$ 443.2043; Found 443.2045 (Δ=0.0002); $[M+Na]^+$ Calcd for $C_{21}H_{26}N_6NaO_5$ 465.1862, Found 465.1861 (Δ=0.0001). This reaction afforded also ethyl 5-ethoxy-2-(furan-2-yl)-[1,2,4]triazolo[1,5-*c*]pyrimidine-8-carboxylate (**50**): white solid; mp 126°C; ^{1}H-NMR (200 MHz, $CDCl_3$) δ 1.46 (3H, t, *J*=7.2 Hz), 1.61 (3H, t, *J*=7.2 Hz), 4.50 (2H, q, *J*=7.2 Hz), 4.87 (2H, q, *J*=7.2 Hz), 6.59 (1H, dd, J=2.1, Hz *J*=4.3 Hz), 7.39 (1H, d, *J*=4.3 Hz), 7.63 (1H, d, *J*=2.1 Hz), 8.68 (1H, s). HRMS (ESI/Q-TOF) m/z:

[M+H]$^+$ Calcd for $C_{14}H_{15}N_4O_4$ 303.1093; Found 303.1097 (Δ=0.0004); [M+Na]$^+$ Calcd for $C_{14}H_{14}N_4NaO_4$ 325.0913, Found 325.0911 (Δ=0.0002).

*Ethyl 5-(2-(tert-butoxycarbonyl)hydrazinyl)-2-(furan-2-yl)-[1,2,4]triazolo[1,5-c]pyrimidine-8-carboxylate (**39**)*: reaction was performed using 260 mg of *tert*-butyl hydrazinecarboxylate (1.98 mmol); yield 15%; white solid; mp 159°C; ^{1}H-NMR (200 MHz, $CDCl_3$) δ 1.41-1.49 (12H, m), 4.49 (2H, q, *J*=7.2 Hz), 6.58-6.60 (1H, m), 7.40 (1H, d, *J*=4.3 Hz), 7.63 (1H, s), 7.94 (1H, bs), 8.71 (1H, s). HRMS (ESI/Q-TOF) m/z: [M+H]$^+$ Calcd for $C_{17}H_{21}N_6O_5$ 389.1573; Found 389.1584 (Δ=0.0011); [M+Na]$^+$ Calcd for $C_{17}H_{20}N_6NaO_5$ 411.1393, Found 411.1393 (Δ=0). This reaction afforded also ethyl 5-ethoxy-2-(furan-2-yl)-[1,2,4]triazolo[1,5-*c*]pyrimidine-8-carboxylate (**50**): see compound 38 synthesis for its charachterization.

~~*Ethyl 5-ethoxy-2-(furan-2-yl)-[1,2,4]triazolo[1,5-c]pyrimidine-8-carboxylate (**50**)*: white solid; mp 126°C; ^{1}H NMR (200 MHz, $CDCl_3$) δ 1.46 (3H, t, *J*=7.2 Hz), 1.61 (3H, t, *J*=7.2 Hz), 4.50 (2H, q, *J*=7.2 Hz), 4.87 (2H, q, *J*=7.2 Hz), 6.59 (1H, dd, J=2.1, Hz *J*=4.3 Hz, J=2), 7.39 (1H, d, *J*=4.3 Hz), 7.63 (1H, d, *J*=2.1 Hz), 8.68 (1H, s). HRMS (ESI/Q-TOF) m/z: [M+H]$^+$ Calcd for $C_{14}H_{15}N_4O_4$ 303.1093; Found 303.1097 (Δ=0.0004); [M+Na]$^+$ Calcd for $C_{14}H_{14}N_4NaO_4$ 325.0913, Found 325.0911 (Δ=0.0002).~~

*General procedure for the removal of tert-butyloxy carbonyl protecting group (compounds **40-42**)*

0.05 mmol of derivatives **37-39** (21 mg of **37**, 22 mg of **38** and 19 mg of **39**) were dissolved in 5 mL of a saturated solution of hydrochloric acid in ethyl acetate. Reaction was stirred at room temperature for 2 hours. Solvent was then removed under reduced pressure and the solid was filtered off to give the desired compounds **40-42**.

*2-(8-Ethoxycarbonyl-2-furan-2-yl-[1,2,4]triazolo[1,5-c]pyrimidin-5-ylamino)-ethyl-amine hydrochloride (**40**)*: yield 75%; white solid; mp 250°C; ^{1}H-NMR (200 MHz, d_6-DMSO) δ 1.35 (3H, t, *J*=7.2 Hz), 3.14 (2H, bs), 3.93 (2H, bs), 4.34 (2H, q, *J*=7.2 Hz), 6.55 (1H, dd, *J*=2.1 Hz, *J*=4.3

Hz), 7.21 (1H, d, *J*=4.3 Hz), 7.61 (1H, d, *J*=2.1 Hz), 8.30 (3H, bs), 8.53 (1H, s). ES-MS m/z: $[M+H]^+$ 317.1.

*Ethyl 2-(furan-2-yl)-5-(piperazin-1-yl)-[1,2,4]triazolo[1,5-c]pyrimidine-8-carboxylate hydrochloride **(41)***: yield quantitative; white solid; mp 270°C; ^{1}H-NMR (200 MHz, D_2O) δ 1.39 (3H, t, *J*=7.2 Hz), 3.50 (4H, bs), 4.36-4.47 (4H, m), 4.79 (2H, under solvent signal), 6.69 (1H, m), 7.28 (1H, d, *J*=3.2 Hz), 7.75 (1H, s), 8.62 (1H, s). HRMS (ESI/Q-TOF) m/z: $[M+H]^+$ Calcd for $C_{16}H_{19}N_6O_3$ 343.1519; Found 343.1519 (Δ=0); $[M+Na]^+$ Calcd for $C_{16}H_{18}N_6NaO_3$ 365.1338, Found 365.1338 (Δ=0.0008).

*Ethyl 2-(furan-2-yl)-5-hydrazinyl-[1,2,4]triazolo[1,5-c]pyrimidine-8-carboxylate hydrochloride **(42)***: yield quantitative; brown solid; mp 146-154°C; ^{1}H-NMR (200 MHz, D_2O) δ 1.39 (3H, t, *J*=7.2 Hz), 4.40 (2H, q, *J*=7.2 Hz), 6.67 (1H, s), 7.26 (1H, s), 7.73 (1H, s), 8.63 (1H, s). ES-MS m/z: $[M+H]^+$ 289.1, $[M+Na]^+$ 311.1.

*Synthesis of 5-(2-tert-Butoxycarbonylamino-ethylamino)-2-furan-2-yl-[1,2,4]triazolo[1,5-c]pyrimidine-8-carboxylic acid **(43)***

To 0.167 mmol of ethyl ester compound **37** dissolved in ethanol was added 1.67 mmol of $LiOH{\cdot}H_2O$ and 1.5 mmol of water. The mixture was refluxed and stirred for three hours. Then, a little amount of water was added and HCl was added since pH 3. The carboxylic acid derivative precipitated and the solid was filtered off. Yield 78%; pale yellow solid; mp 150°C; ^{1}H-NMR (400 MHz, d_6-DMSO) δ 1.30 (9H, s), 3.22 (2H, m), 3.68 (2H, m), 6.75 (1H, dd, *J*=2.1 Hz, *J*=4.3 Hz), 6.92 (1H, bs), 7.26 (1H, d, J=4.3 Hz), 7.97 (1H, d, *J*=2.1 Hz), 8.53 (1H, s), 9.00 (1H, bs), 12.75 (1H, bs). ES-MS m/z: $[M+Na]^+$ 411.1.

Biology

Binding at the human A_1, A_{2A} and A_3 ARs

All pharmacological methods followed the procedures as described earlier.[22] Briefly, membranes for radioligand binding were prepared from CHO cells stably transfected with human AR subtypes

in a two-step procedure. In a first low-speed step (1,000 x g), cell fragments and nuclei were removed, thenthe crude membrane fraction was sedimented from the supernatant at 100,000 x g. The membrane pellet was resuspended in the buffer used for the respective binding experiments (50 mMTris/HCl buffer pH 7.4 for hA_1 and hA_{2A} AR; 50 mMTris/HCl,10 mM $MgCl_2$, 1 mM EDTA, pH 8.25 for hA_3-AR), frozen in liquid nitrogen and stored at -80 °C. For radioligand binding at the hA_1 AR 1 nM [^{3}H]CCPA was used, whereas 10 nM [^{3}H]NECA and 1 nM [^{3}H]HEMADO were used for hA_{2A} and hA_3 ARs, respectively. Non specific binding of [^{3}H]CCPA was determined in the presence of 1 mM theophylline, in the case of [^{3}H]NECA and [^{3}H]HEMADO, 100 µM R-PIA was used.[22][23][24]K_i-values from competition experimentswere calculated with the program SCTFIT. [25]

Adenylyl cyclase activity

The potency of antagonists at the hA_{2B}-AR was determined in adenylyl cyclase experiments. The procedure was carried out as described previously with minor modifications. [22][26] In this case only one high speed centrifugation of the homogenate of CHO cells stably transfected with human A_{2B}-AR subtypes was used. The resulting crude membrane pellet was resuspended in 50 mMTris/HCl, pH 7.4 and immediately used for the cyclase assay. Therefore, inhibition of NECA-stimulated adenylyl cyclase activity (stimulation with 5 µM of NECA) was determined as a measurement of affinity of compounds. Membranes were incubated with about 150,000 cpm of [α-^{32}P]ATP for 20 min in the incubation mixture as described without EGTA and NaCl. [26] IC_{50} values were calculated with the Hill equation. Hill coefficients in all experiments were near unity.

Molecular modelling

Software overview

Molecular modeling studies were performed on a 8 CPU (Intel® Xeon® CPU E5-1620 3.50GHz) linux workstation. General molecular modeling operations were executed using the MOE suite (Molecular Operating Enviroment, version 2018.01) [27].

GOLD (Genetic Optimization for Ligand Docking, version 5.4.1) [28] suite was used as docking program, and the collected poses were analyzed (energy computation and visual inspection) through MOE.

Three-dimensional structures of Adenosine Receptors

A crystallographic structure was retrieved from the Protein Data Bank for hA_{2A} and hA_1 adenosine receptors, resulting in structure 3PWH [21] and 5UEN [20], respectively. Among the various crystallographic structures available for hA_{2A}–AR, one complex with the inverse agonist ZM-241385 was chosen, because of the chemical similarity of its 7-amino[1,2,4]triazolo[1,5,*a*][1,3,5]triazine scaffold with the 5-amino[1,2,4]triazolo[1,5-*c*]pyrimidine moiety of the compounds under investigation.

Given the lack of any crystallographic structures for hA_3-AR, a homology model was retrieved from the *Adenosiland* web-platform [29][30] previously developed by our research group. The model was constructed using 3PWH as a template, considering the presence of ZM-241385 as environment for induced fit.

The residues of ARs are identified according the generic Ballesteros Weinstein numbering system [31] throughout this work.

Molecular docking

Three dimensional structures of the ligands were built by the MOE-builder tool. Ionization states were predicted using the MOE-protonate 3D tool [32]. Tautomers and atom hybridation were checked, and structures were minimized by the MMFF94x until the root mean square (RMS) gradient fell below 0.1 kcal mol^{-1} A^{-1}. GOLD docking tool was selected as a conformational search program and Goldscore as scoring function, referring to a previous docking benchmark study performed by our team [33] [34]. For each ligand, 20 docking simulation runs were performed on each receptor subtype, searching on a sphere of 20 Å radius, centered on the lateral chain nitrogen of the conserved N6.55.

Docking Analysis

Ligand and protein partial charges were calculated using the PM3 [35] method and AMBER12EHT force field respectively. Then, electrostatic and Van der Waals energy contributions to the binding energy were calculated by MOE, together with per residue electrostatic and hydrophobic interactions. Per residue information were reported in the so-called "Interaction Energy Fingerprints" (IEF) [33]: they consists in heat maps reporting the strength of the interaction of each residue (x-axis) and each ligand (y-axis) according to a colorimetric scale going from blue to red for negative to positive values in the case of electrostatic contributions (IEFele), and from white to dark green for low to high values for hydrophobic contributions (IEFhyd). The interactions of most relevant residues were also reported in histograms, whose height is proportional to the strength of the interaction. All the plots were produced using GNUPLOT 4.6 [36].

MMSDocking Video Maker

The in-house MMsDocking video maker tool was exploited to produce videos showing the docking poses, per residue IEFhyd and IEFele data for selected residues, experimental binding data and scoring values. Representations of docking poses were produced using CHIMERA52 [37], two-dimensional depictions were constructed through the cheminformatics toolkit RDKit [38], the heat maps were obtained through GNUPLOT 4.6 [36]; in the end, videos were mounted using MEncoder [39].

Acknowledgments

MMS lab is very grateful to Chemical Computing Group, OpenEye, and Acellera for the scientific and technical partnership. MMS lab gratefully acknowledges the support of NVIDIA Corporation with the donation of the Titan Xp GPU used for this research.

References

[1] B.B. Fredholm, A.P. IJzerman, K.A. Jacobson, K.-N. Klotz, J. Linden, International ~~U~~union of p~~P~~harmacology . XXV . Nomenclature and c~~C~~lassification of a~~A~~denosine r~~R~~eceptors, Pharmacol. Rev. 53 (2001) 527–552.

[2] B.B. Fredholm, Adenosine — a physiological or pathophysiological agent ?, J. Mol. Med. 92

Formattato: Giustificato

(~~2013~~2014) 201-6. doi:10.1007/s00109-013-1101-6.

[3] B.B. Fredholm, A.P. IJzerman, K.A. Jacobson, J. Linden, C.E. Mu, International u~~U~~nion of b~~B~~asic and c~~C~~linical p~~P~~harmacology . LXXXI . Nomenclature and c~~C~~lassification of a~~A~~denosine r~~R~~eceptors — An u~~U~~pdate, Pharmacol. Rev. 63 (2011) 1–34. doi:10.1124/pr.110.003285.1.

[4] K.A. Jacobson, Z. Gao, Adenosine receptors as therapeutic targets, Nat. Rev. Drug Discov. 5 (2006) 247–~~2~~64. doi:10.1038/nrd1983.

[5] V. Mitrovic, P. Seferovic, S. Dodic, M. Krotin, A. Neskovic, K. Dickstein, H. De Voogd, C. Böcker, D. Ziegler, M. Godes, R. Nakov, H. Essers, C. Verboom, B. Hocher, Cardio-renal effects of the A_1 adenosine receptor antagonist SLV320 in patients with heart failure, Circ. Hear. Fail. 2 (2009) 523–~~5~~31. doi:10.1161/CIRCHEARTFAILURE.108.798389.

[6] S.C. Yap, H.T. Lee, Adenosine and protection from acute kidney injury, Curr. Opin. Nephrol. Hypertens. 21 (2012) 24–32. doi:10.1097/MNH.0b013e32834d2ec9.~~Adenosine.~~

~~[7] P.A. Borea, K. Varani, F. Vincenzi, P.G. Baraldi, M.A. Tabrizi, S. Merighi, S. Gessi, The A3 Adenosine Receptor: History and Perspectives, Pharmacol. Rev. 67 (2014) 74–102. doi:10.1124/pr.113.008540.~~

[7] D. Preti, P.G. Baraldi, A.R. Moorman, P.A. Borea, K. Varani, History and perspectives of A_{2A} adenosine receptor antagonists as potential therapeutic agents., Med. Res. Rev. 35 (2015) 790–848. doi:10.1002/med.21344.

[8] R.M. Brown, J.L. Short, Adenosine A_{2A} receptors and their role in drug addiction, J. Pharm. Pharmacol. 60 (2008) 1409–1430. doi:10.1211/jpp/60.11.0001.

[9] B. Cacciari, G. Pastorin, C. Bolcato, G. Spalluto, M. Bacilieri, S. Moro, A~~–~~$_{2B}$ adenosine receptor antagonists : recent developments, Mini-Reviews Med. Chem. 5 (2005) 1053–~~10~~60.

[10] K. Sun, Y. Xia, New insights into sickle cell disease: a disease of hypoxia., Curr. Opin. Hematol. 20 (2013) 215–21. doi:10.1097/MOH.0b013e32835f55f9.

[11] S.L. Cheong, S. Federico, G. Venkatesan, A.L. Mandel, Y. Shao, S. Moro, G. Spalluto, G.

Formattato: Pedice

Formattato: Rientro: Sinistro: 0 cm, Prima riga: 0 cm

Formattato: Giustificato

Formattato: Pedice

Formattato: Pedice

Formattato: Pedice

Pastorin, The A_3 ~~Adenosine~~ adenosine r~~R~~eceptor as m~~M~~ultifaceted t~~T~~herapeutic t~~T~~arget : ~~P~~pharmacology , m~~M~~edicinal c~~C~~hemistry , and i~~I~~n s~~S~~ilico a~~A~~pproaches, Med. Res. Rev. 31 (2011). doi:10.1002/med.20254.

[12] K.A. Jacobson, A.M. Klutz, D.K. Tosh, A.A. Ivanov, D. Preti, Medicinal c~~C~~hemistry of the A_3 ~~A~~adenosine r~~R~~eceptor: a~~A~~gonists, a~~A~~ntagonists, and r~~R~~eceptor e~~E~~ngineering, Handb. Exp. Pharmacol. 193 (2009) 123–~~1~~59. doi:10.1007/978-3-540-89615-9.

[13] CF101 clinical trials, https://clinicaltrials.gov/ct2/results?term=CF101&Search=Search.

[14] CF102 clinical trials, https://clinicaltrials.gov/ct2/results?term=CF102&Search=Search.

[15] Palobiofarma SL, "First-in-human" s~~S~~tudy t~~T~~o a~~A~~ssess the s~~S~~afety and t~~T~~olerability of PBF-677 in h~~H~~ealthy v~~V~~olunteers, (2016). https://clinicaltrials.gov/ct2/show/NCT02639975?term=A3+antagonist&rank=1.

[16] S. Federico, A. Ciancetta, N. Porta, S. Redenti, G. Pastorin, B. Cacciari, K.-N. Klotz, S. Moro, G. Spalluto, Scaffold decoration at positions 5 and 8 of 1,2,4-triazolo[1,5-*c*]pyrimidines to explore the antagonist profiling on adenosine receptors: A preliminary structure-activity relationship study, J. Med. Chem. 57 (2014) 6210–~~62~~25. doi:10.1021/jm500752h.

[17] H. Tsumuki, J. Shimada, H. Imma, A. Nakamura, H. Nonaka, S. Shiozaki, S. Ichikawa, T. Kanda, Y. Kuwana, M. Ichimura, F. Suzuki, [1,2,4]triazolo[1,5-*c*]pyrimidine derivatives, EP0976753A1, 2000.

[18] S. Federico, A. Ciancetta, D. Sabbadin, S. Paoletta, G. Pastorin, B. Cacciari, K.-N. Klotz, S. Moro, G. Spalluto, Exploring the d~~D~~irectionality of 5-s~~S~~ubstitutions in a n~~N~~ew s~~S~~eries of 5-a~~A~~lkylaminopyrazolo[4,3-~~–~~*e*~~–~~]1,2,4-triazolo[1,5-~~–~~*c*~~–~~]pyrimidine as a ~~S~~strategy t~~T~~o ~~D~~design ~~N~~novel h~~H~~uman A_3 ~~Adenosine~~ adenosine ~~Receptor~~ receptor ~~Antagonists~~antagonists., J. Med. Chem. 55 (2012) 9654–~~96~~68. doi:10.1021/jm300899q.

[19] E. Kozma, T.S. Kumar, S. Federico, K. Phan, R. Balasubramanian, Z.-G. Gao, S. Paoletta, S. Moro, G. Spalluto, K.A. Jacobson, Novel fluorescent antagonist as a molecular probe in A

Formattato: Pedice
Formattato: Pedice
Formattato: Giustificato
Formattato: Tipo di carattere: Corsivo
Formattato: Tipo di carattere: Corsivo
Formattato: Giustificato
Formattato: Tipo di carattere: Corsivo
Formattato: Tipo di carattere: Corsivo
Formattato: Pedice
Formattato: Pedice

~~<inf>~~3~~</inf>~~ adenosine receptor binding assays using flow cytometry, Biochem. Pharmacol. 83 (2012) 1552–61. doi:10.1016/j.bcp.2012.02.019.

[20] A. Glukhova, D.M. Thal, A.T. Nguyen, E.A. Vecchio, M. Jörg, P.J. Scammells, L.T. May, P.M. Sexton, A. Christopoulos, Structure of the a~~A~~denosine A_1 ~~Receptor~~ receptor reveals the basis for subtype selectivity, cell. 168 (2017) 867–~~8~~77.e13. doi:10.1016/j.cell.2017.01.042.

[21] A.S. Doré, N. Robertson, J.C. Errey, I. Ng, K. Hollenstein, B. Tehan, E. Hurrell, K. Bennett, M. Congreve, F. Magnani, C.G. Tate, M. Weir, F.H. Marshall, Structure of the adenosine A_{2A} receptor in complex with ZM241385 and the xanthines XAC and caffeine, Structure~~.~~ 19 (2011) 1283–~~12~~93. doi:10.1016/j.str.2011.06.014.

[22] K.-N. Klotz, J. Hessling, J. Hegler, C. Owman, B. Kull, B.B. Fredholm, M.J. Lohse, Comparative pharmacology of human adenosine receptor subtypes -~~-~~ characterization of stably transfected receptors in CHO cells, Naunyn. Schmiedebergs. Arch. Pharmacol. 357 (1998) 1–9. doi:10.1007/PL00005131.

[23] K.-N. Klotz, E. Camaioni, R. Volpini, S. Kachler, S. Vittori, G. Cristalli, 2-Substituted N -ethylcarboxamidoadenosine derivatives as high-affinity agonists at human A_3 adenosine receptors, Naunyn. Schmiedebergs. Arch. Pharmacol. 360 (1999) 103–~~10~~8. doi:10.1007/s002109900044.

[24] K.-N. Klotz, N. Falgner, S. Kachler, C. Lambertucci, S. Vittori, R. Volpini, G. Cristalli, [^{3}H]HEMADO- a novel tritiated agonist selective for the human adenosine A_3 receptor, Eur. J. Pharmacol. 556 (2007) 14–~~1~~8. doi:10.1016/j.ejphar.2006.10.048.

[25] A. De Lean, A.A. Hancock, R.J. Lefkowitz, Validation and statistical analysis of a computer modeling method for quantitative analysis of radioligand binding data for mixtures of pharmacological receptor subtypes, Mol. Pharmacol. 21 (1982) 5–16.

[26] K.-N. Klotz, G. Cristalli, M. Grifantini, Photoaffinity labeling of A_1-adenosine receptors, J. Biol. Chem. 260 (1985) 14659–14664.

[27] Chemical Computing Group ULC, MOE, Mol. Oper. Environ. Available from:

Formattato: Pedice

Formattato: Giustificato

Formattato: Pedice

Formattato: Pedice

Formattato: Apice

Formattato: Pedice

Formattato: Pedice

http://www.chemcomp.com

[28] The Cambridge Crystallographic Data Centre (CCDC), Genetic Optimization for Ligand Docking (GOLD),. Available from: https://www.ccdc.cam.ac.uk/solutions/csd-discovery/components/gold/

[29] M. Floris, D. Sabbadin, R. Medda, A. Bulfone, S. Moro, ~~European Journal of Medicinal Chemistry~~ Adenosiland : Walking through adenosine receptors landscape, Eur. J. Med. Chem. 58 (2012) 248–~~2~~57. doi:10.1016/j.ejmech.2012.10.022.

[30] M. Floris, D. Sabbadin, A. Ciancetta, R. Medda, A. Cuzzolin, S. Moro, Implementing the "Best Template Searching" tool into Adenosiland platform~~.~~, Silico Pharmacol. 1 (2013) 25. doi:10.1186/2193-9616-1-25.

[31] J.A. Ballesteros, H. Weinstein, Integrated methods for the construction of three-dimensional models and computational probing of structure-function relations in G protein-coupled receptors, Methods Neurosci. 25 (1995) 366–428. doi:10.1016/S1043-9471(05)80049-7.

[32] P. Labute, Protonate3D: Assignment of ionization states and hydrogen coordinates to macromolecular structures, Proteins Struct. Funct. Bioinforma. 75 (2009) 187–205. doi:10.1002/prot.22234.

[33] A. Ciancetta, A. Cuzzolin, S. Moro, Alternative quality assessment strategy to compare performances of GPCR-ligand docking protocols: The human adenosine A_{2A} receptor as a case study, J. Chem. Inf. Model. 54 (2014) 2243–~~22~~54. doi:10.1021/ci5002857.

[34] A. Cuzzolin, M. Sturlese, I. Malvacio, A. Ciancetta, S. Moro, DockBench: An integrated informatic platform bridging the gap between the robust validation of docking protocols and virtual screening simulations, Molecules. 20 (2015) 9977–~~99~~93. doi:10.3390/molecules20069977.

[35] J.J.P. Stewart, Optimization of parameters for semiempirical methods V: Modification of NDDO approximations and application to 70 elements, J. Mol. Model. 13 (2007) 1173–~~1~~213. doi:10.1007/s00894-007-0233-4.

Formattato: Pedice

[36] Gnuplot. Available from: http://www.gnuplot.info/index.html

[37] E.F. Pettersen, T.D. Goddard, C.C. Huang, G.S. Couch, D.M. Greenblatt, E.C. Meng, T.E. Ferrin, UCSF Chimera - A visualization system for exploratory research and analysis, J. Comput. Chem. 25 (2004) 1605–~~16~~12. doi:10.1002/jcc.20084.

[38] RDKit: Cheminformatics and Machine Learning Software. Available from: http://www.rdkit.org

[39] MEncoder. Available from: http://www.mplayerhq.hu/design7/projects.html

Formattato: Giustificato